Design Engineering of Energy and Geo-Environmental Systems
EGEE 580

CAPTURE, SEQUESTRATION, AND UTILIZATION OF CARBON DIOXIDE FROM POWER GENERATION PLANT

Bander N. Al Ghamdi
Kyungsoo Kim
Seyhan Emre Gorucu
Yogesh Bansal

SPRING 2009

TABLE OF CONTENTS

List of Figures

List of Tables

Chapter 1

Introduction

1.1 Overview

Increasing level of Green-House-Gases (GHGs) is posing a threat on the atmosphere of the earth. These GHGs absorbs infra-red radiations and trap heat that results in increased temperature levels of the environment. GHGs are categorized into naturally occurring gases (water vapor, carbon dioxide, methane, and nitrous oxide) and anthropogenic gases (industrial gases like CFC*, emission of CO_2 etc). If the levels of GHGs keep on increasing with time in the atmosphere then amount of radiations absorbed in the atmosphere would be more and the Earth's temperature will keep on increasing. On the other hand if concentration of GHG remains stable then the amount of energy radiated back by Earth's atmosphere will be same the amount of energy absorbed by the Earth's atmosphere, which would maintain the temperature of the Earth's surface roughly constant, though higher than the current average temperature [3.1]. With rapid industrialization in the past century, the use of fossil fuel increased with time and the due to the same reason the level of carbon dioxide has continuously increased in the atmosphere. The trend of increase in the CO_2 level can be seen in Figure 1.

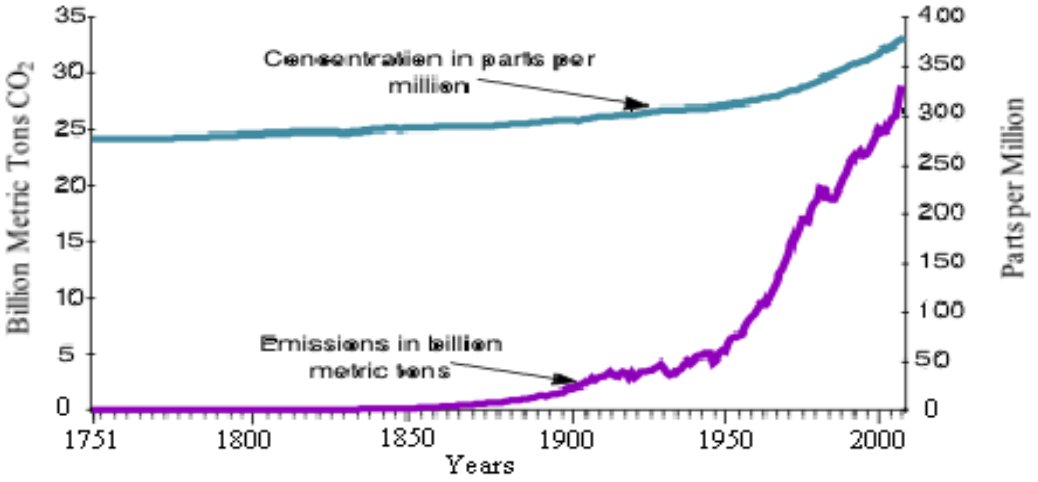

Source: Oak Ridge National Laboratory, Carbon Dioxide Information Analysis Center

Figure 1: CO2 emission and concentration

* Chloro Floro Carbons

During 2007, global emission of carbon was 7 billion tons which is expected to increase to 14 giga tons per year by the year 2050 assuming the demand for fossil fuel keeps increasing because of the growing economies around the world [3.2]. There has been a direct relationship between the amount of carbon dioxide emission and the amount of fossil fuel consumption to improve our day to day life. A comparison of Figure 1 and Figure 2 shows the same relationship. The steep trend of fossil fuel consumption can be seen in carbon dioxide emission during the last 40-50 years.

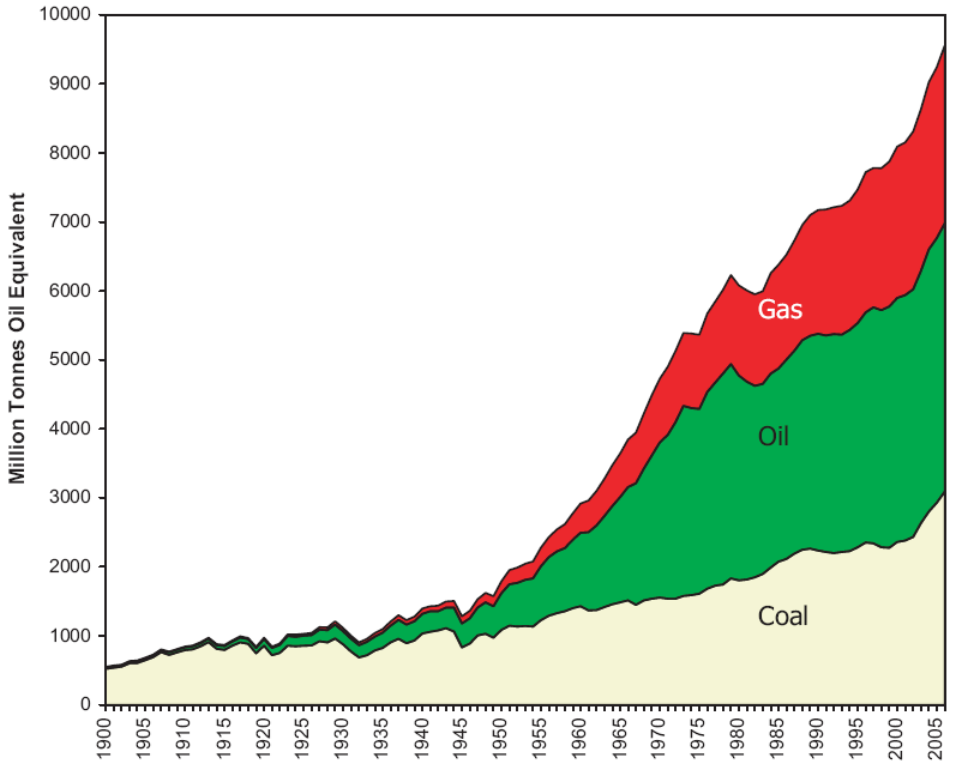

Figure 2: Trend of energy consumption in the past century (source: Bryant S. 2007[2])

Among all the GHGs produced CO_2 is the largest emitted gas with a total contribution of 83.8% of the total gases emitted in United States in 2006. Other gases include methane, nitrous oxide, hydrofloro carbons (HFCs), perfloro carbons (PFCs) and sulfur hexa-floride (SF_6). The emission distribution of each gas in 2006 is shown in Figure 3. CO_2 is the largest contributor in global warming of the environment. Therefore, measures must be taken in order to control the concentration of these gases in the atmosphere which can be done in two ways. First, increase the efficiency of the fuel usage that will slow down the GHGs emission as less fuel will be required for the same work. Secondly, GHGs must be captured and then either sequestered or utilized. In this project, capturing of CO_2, sequestration in exhausted oil/gas field and saline aquifer, and utilization of CO_2 is studied.

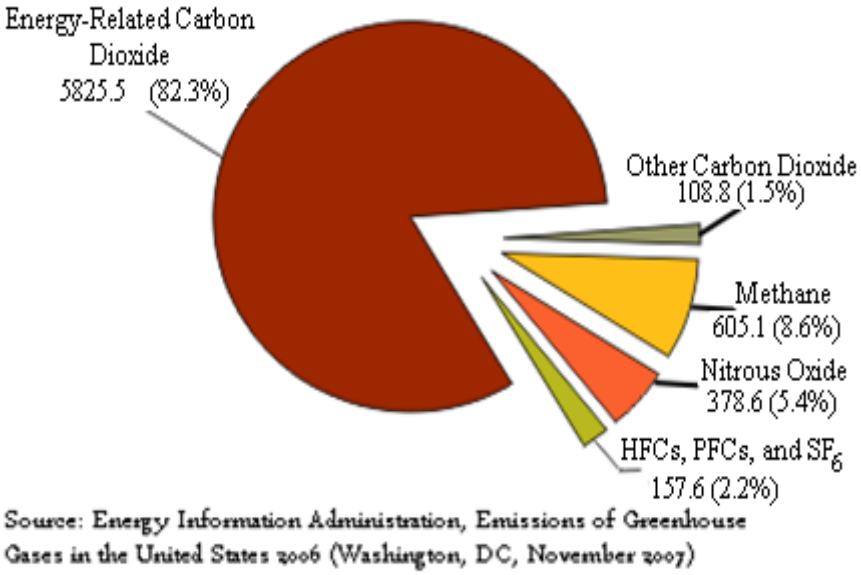

Figure 3: GHGs distribution in United States of America (Million Metric Tons of CO2 Equivalent)

1.2 Team Statement

A study will be conducted on a coal fired power plant located in Pennsylvania to develop a plan to efficiently capture CO_2, sequester, and utilize it for industrial purposes while considering technical and economical analysis. The intention of this project is to eliminate the emission of CO_2 into the atmosphere by achieving the following goals:

- Find out a proper CO2 capture method for Pennsylvania
- Investigate the effects of CO2 capture process implementation on plant efficiency and electricity production cost
- Estimate the cost for CO2 capture
- Find an optimized injection rate of CO2
- Estimate leakage in the system
- Estimate the cost of CO2 that should be charged in order to recover the capital cost in 10 years
- Carry out a transportation analysis
- Calculate the trapping capacity
- Estimate the flow using the pressure profile
- Address implementations of CO2 in EOR technology
- Review current CO2-EOR schemes and limitations
- Adapt an EOR method and draw engineering and economical analysis

Chapter 2

CO_2 Capture

2.1 Introduction

Greenhouse gas mitigation is an issue for which a world-wide effort is needed. CO_2, which is one of the greenhouse gases, mostly comes from burning fossil fuels, and almost 85% of world's commercial energy consumption depends on fossil fuel. The energy demand will even increase by 57% from 2004 to 2030 according to EIA report. To reduce CO_2 emission, various CO_2 mitigation technologies were invented, and there are three main options for power plant-scale use: Post-combustion, Pre-combustion, and Oxy-fuel combustion. Different technologies can be applied to different power plants considering types of flue gas stream. Coal-fired power plant, for instance, which is responsible for almost 30% of CO_2 emission in the U.S, are good targets to apply these technologies [2.2]. Almost 75 percent of total carbon capture and sequestration (CCS) cost stems from CO_2 capture, and this whole processes increase the electricity production cost by 50 percent [2.3]. Cost reduction for CCS technology is one of the most important issues and can be achieved by analyzing details of each CCS technique and proper application of them.

Table 1: Comparison of power stations with and without CO2 capture (International Energy Agency Greenhouse Gas Programme, 2006a)

Technology	Thermal efficiency (% LHV)	Capital cost ($/kW)	Electricity cost (c/kWh)	Cost of CO2 Avoided ($/tCO2)
Coal-fired plants				
No capture	44	1410	5.4	
Post-combustion	34.8	1980	7.5	34
Pre-combustion	31.5	1820	6.9	23
Oxy-fuel	35.4	2210	7.8	36

2.2 Capturing Methods

2.2.1. Post-combustion

CO_2 in the flue gas from coal combustion is captured in the system. Coal-fired power plants usually generate below 15% CO_2 by concentration so that post-combustion process cost is mainly determined by capture unit for its low partial pressure(less than 0.15 atm) and subsequent

low driving force [2.5]. Since almost 70% of the process cost is spent for the capturing unit, developing new capture processes and improving current techniques are of most important [2.6]. Although post-combustion system has some difficulties, it is still one of the most promising techniques because of it easy implementation. The system can be implemented to almost all existing power plants which are responsible for almost 65% of CO_2 emission as well as industrial plants (chemical plants, glass, refineries, cement, steel, etc.) [2.5][2.6]. Current techniques for post-combustion are absorption with solvent, adsorption, and membrane separation.

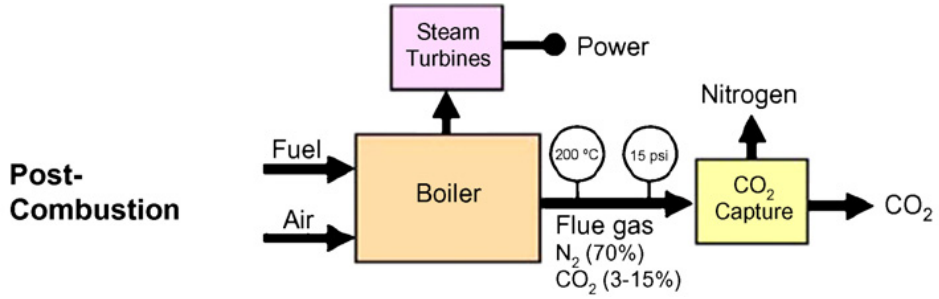

Figure 4: Schematic of Post-Combustion [2.5]

2.2.2 Pre-combustion

In the system, synthetic gas (hydrogen and carbon monoxide) is produced by coal gasification, and the synthetic gas can be used to generate electricity in gas turbine or be converted into CO_2 and H_2 through water-gas shift reaction. Among a wide variety of CO_2 capturing technologies, absorption method, which has two types of processes, is the most widely used technology for gasification power plants. In chemical absorption, solvent reacts with CO_2 chemically, and the solution is separated back in regenerator. In physical absorption, however, CO_2 and solvent react physically with some pressure increase [2.7]. According to the department of energy in the U.S, electricity production cost will increase by 25% for the application of capturing unit. The goal of reducing the cost increase to 10% has been set [2.7]. Unlike post-combustion method, the CO_2 concentration and pressure of flue gas stream is typically high, there is no need to pressurize the feed, which allows significant energy saving. Pre-combustion method, however, can be applied to only fossil fuel power plants.

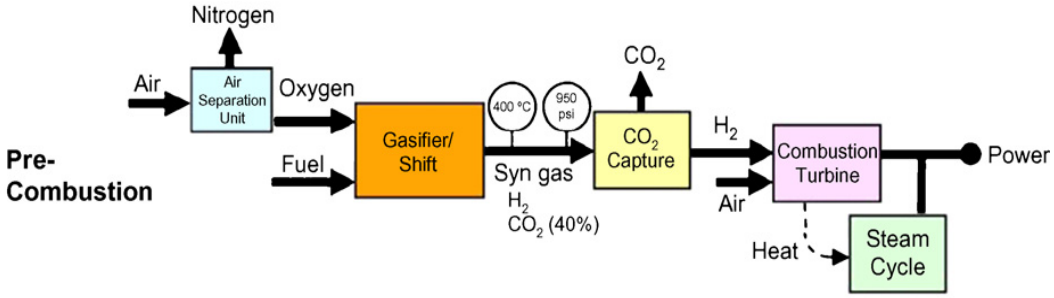

Figure 5: Schematic of Pre-Combustion [2.5]

2.2.3 Oxy-fuel Combustion

In oxy-fuel combustion, air separation unit (ASU) is applied to pulverized coal-fired power plant with CO_2 recovery system. Since oxygen is the only element involved in combustion, there is no nitrogen in the flue gas, and NOX control unit is not necessary. In oxy-fuel combustion, sulfur compounds are removed first, and CO2 concentration in flue gas becomes 90%. After water in flue gas is removed through condensation by cooling down the stream, CO_2 concentration increase to around 95% [2.4][2.9]. No further CO_2 separation process is needed and the concentrated CO_2 is then compressed for storage. In this technology, a smaller sized boiler can be used because coal combustion occurs under only oxygen-existing environment. The size of other equipments can be reduced as well. However, the equipment corrosion caused by increased SO_2 concentration in the flue gas can be an issue. Oxy-fuel combustion technique is not mature enough to be used for practical purposes for the following reasons: the capital cost, which is around USD $2,040/kW, is high compared to the other techniques [2.7], and the air separation unit would consume 23% to 37% of the energy coming from a power plant, which causes significant efficiency loss [2.4]. A method to apply oxy-fuel combustion to gasification power plants using a gas turbine is under development [2.10].

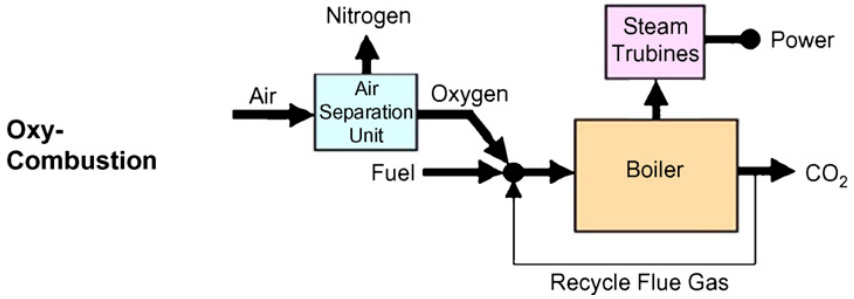

Figure 6: Schematic of Oxy-fuel Combustion [2.5]

Table 2: Advantages and disadvantages of different CO2 capture approaches [2.5]

	Advantages	Barriers to implementation
Post-combustion	• Applicable to the majority of existing coal-fired power plants • Retrofit technology option	Flue gas is … • Dilute in CO_2 • At ambient pressure … resulting in … • Low CO_2 partial pressure • Significantly higher performance or circulation volume required for high capture levels • CO_2 produced at low pressure compared to sequestration requirements
Pre-combustion	Synthesis gas is … • Concentrated in CO_2 • High pressure … resulting in … • High CO_2 partial pressure • Increased driving force for separation • More technologies available for separation • Potential for reduction in compression costs/loads	• Applicable mainly to new plants, as few gasification plants are currently in operation • Barriers to commercial application of gasification are common to pre-combustion capture • Availability • Cost of equipment • Extensive supporting systems requirements
Oxy-combustion	• Very high CO_2 concentration in flue gas • Retrofit and repowering technology option	• Large cryogenic O_2 production requirement may be cost prohibitive • Cooled CO_2 recycle required to maintain temperatures within limits of combustor materials • Decreased process efficiency • Added auxiliary load

In this work, post-combustion method will be used to investigate the effects of CO2 capture on power plant efficiency and electricity production cost. From the technique's relatively low capital cost, easy implementation, and technical feasibility, we concluded that post-combustion method is the most proper one. The dominance of coal-fired power plant in Pennsylvania also supports the conclusion by eliminating pre-combustion method, which can be used for gasification power plants, from candidate capturing methods. You can find more information about power plants in Pennsylvania in chapter 2.4

2.3 Options for Post-combustion Method

2.3.1 Absorption

Figure 7 shows a schematic of absorption process. The flue gas enters an absorber after passing through a pre-washer which is used to cool down the stream. The solvent is regenerated in the regenerator at high temperature and high pressure. Water vapor is condensed at the top of the regenerator, resulting in almost pure CO_2 yield. To prevent solvent loss, additional washing systems are installed on both absorber and regenerator [2.12]. The most widely used solvent is

monoethanolamine (MEA). There are several reasons why CO_2 absorption process with amine is most reliable for combustion-based power plants [2.2].

(1) Amine-based CO_2 capture system is effective for streams with low CO_2 concentration, such as flue gases from coal combustion, which contain only 10% ~ 12% CO_2 by volume.
(2) The systems is available for commercial purpose and has been used for a long time.
(3) The system is similar to other pipe-end control systems used for power plants. Operating conditions are ordinary pressure and temperature.
(4) There is a worldwide effort to improve the system. Thus, more improved technologies will be available in the future.

Absorption is also favored in other industry sectors: many other commercial power plants are using amine-based CO_2 capture process to handle CO_2 emission [2.6].

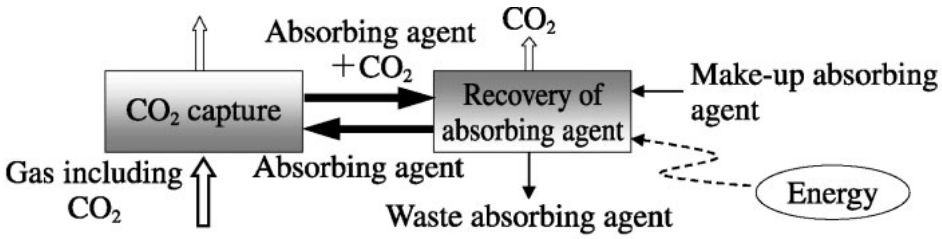

Figure 7: Absorption capture method [2.9]

2.3.1.1 Economy

In absorption method, the flue gas flow rate in the system and energy consumption for solvent regeneration mainly determines the operating cost and the efficiency of power plants. To apply this technology in the future, cost reduction by process and solvent improvements must be achieved first. For example, optimizing the solvent concentration and the solvent regenerator operating temperature and pressure can reduce the process cost significantly. For a pulverized coal power plant, the increase in cost of electricity production by adopting CO_2 capture process is estimated to be 40~85%. The cost of capturing CO_2 can be calculated as

$$\text{Cost of } CO_2 \text{ avoided (\$/ton)} = \frac{\text{Cost of electricity(capture)} - \text{Cost of electricity(reference)}}{\text{CO2 emission(refrence)} - \text{CO2 emission(capture)}}$$

From the equation above, the electricity production cost for power plants with CO_2 capture process is US$ 0.04 to 0.09 per kWh, whereas, the cost is US$ 0.03–0.06 per kWh for the plants without the capture process [2.11]. Capital cost of the CO_2 capturing unit is another factor to influence electricity production cost. In the capturing unit absorber is the most expensive equipment which accounts for 55% of total capital cost, and the solvent regenerator is the second expensive equipment which is responsible for 17% of the capital cost. A cheap and improved

material or a simplified capture system can reduce the cost for equipment purchase significantly [2.11]. Optimizing the diameters and heights of the absorber and the solvent regenerator column which is influenced by flue gas flow rate can reduce capital cost [2.12].

2.3.1.2 Efficiency

The addition of CO_2 the absorption process significantly decreases the efficiency of a power plant; when capturing 85% of CO_2 from flue gas, the efficiency drops about 14%, which is mainly caused by the heat loss in the solvent regeneration process, and the heat comes from low-pressure steam within the power plant [2.11]. Electrical energy is also needed to compress CO_2 product and to pump flue gas and solvent, also decreasing the efficiency of a power plant [2.2].

2.3.1.3 Technical Limitation

There are some issues to be solved for proper application of absorption CO_2 capture method. First, hazardous wastes from the capture system may cause environmental problems. Ammonia gas is generated during the capture process by degradation of MEA solvent, and some other dangerous solid wastes are also produced at the bottom of solvent regenerator during solvent recovery [2.2]. Second, chemical and thermal degradation of solvent affect the efficiency of CO_2 capture process by reducing amine fraction of the solvent. The amount of oxygen in the flue gas is from 3% to13% depending on the types of power plants. Thermal degradation can occur in a form of solvent oxidation by solvent contacting with oxygen at the temperature of 40~608℃. Chemical degradation can occur when NO_2 and SO_2, acid gases, in the flue gas block the functions of the solvent irreversibly [2.12]. Last, a small portion of the toxic solvent can leave the regenerator with recovered CO_2 flow stream during the solvent regeneration process. The amount of the solvent leaving the regenerator is estimated to be 10g/ton CO_2 captured [2.13].

2.3.2 Membrane

In membrane method, CO_2 is captured through interactions between components in the flue gas and the membrane material. Because each component in the flue gas has a different degree of interaction between the membranes, CO_2 is more likely to dissolve into the membrane and diffuse through it. Membrane method can be a promising future CO_2 capture technique because it requires very small energy for CO_2 capture and has high performance. In addition, the membrane process allows space saving and is easy to scale up. However, high flue gas flow rate and high selectivity and high stability of membrane, which are required for membrane working properly, are not easy to achieve with current technology [2.4][2.9][2.14].

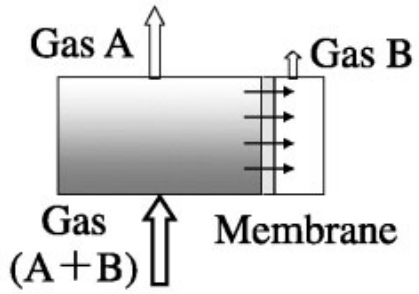

Figure 8: Membrane capture method [2.9]

2.3.2.1 Economy

To achieve high flue gas flow rate needed for the membrane capture system to work properly, the system needs a compressor which is responsible for up to 80% of the total capital. The size of membrane increases as CO_2 capture rate increases, which accounts for 10% of the capital cost. The cost for membrane size increase is only a small portion of the capital cost compared to the cost for the compressor. Thus, the total capital cost will not change much even if the cost for membrane increases due to higher CO_2 capture rate, which leads to the fact that the cost per ton of CO_2 captured drops as the captured amount increases to a certain limit. That is, there is a certain amount of captured CO_2 which should be achieved to minimize total capital cost for membrane process [2.14].

2.3.2.2 Efficiency

The selectivity of membrane determines the degree of each component in flue gas passing through the membrane. A membrane with high selectivity for CO_2 gives a purer captured CO_2 stream. The permeability of membrane, however, decreased as the selectivity increases resulting in the lower flow rate of the stream through membrane. Thus, an optimized balance between the purity of stream and the amount of stream is needed [2.14]. Since membrane capture process does not require heat for solvent regeneration, which decreases the efficiency of a power plant by 14%, it shows better efficiency [2.11]. However, specific conditions should be satisfied first for the case to be valid.

2.3.2.3 Technical Limitation

In membrane process, high pressure and high CO_2 concentration are needed for enough driving force for CO_2 stream to pass through membrane and to be separated. Therefore, the flue gas needs to be compressed until it reaches to enough driving force at least 10 bar in total (Bailey and Feron, 2005), where permeability of each component in flue gas is known [2.15]. In addition, the selectivity of membrane needs to be increased by 50%. The selectivity of current membrane is not high enough for the capture process to work properly [2.6]

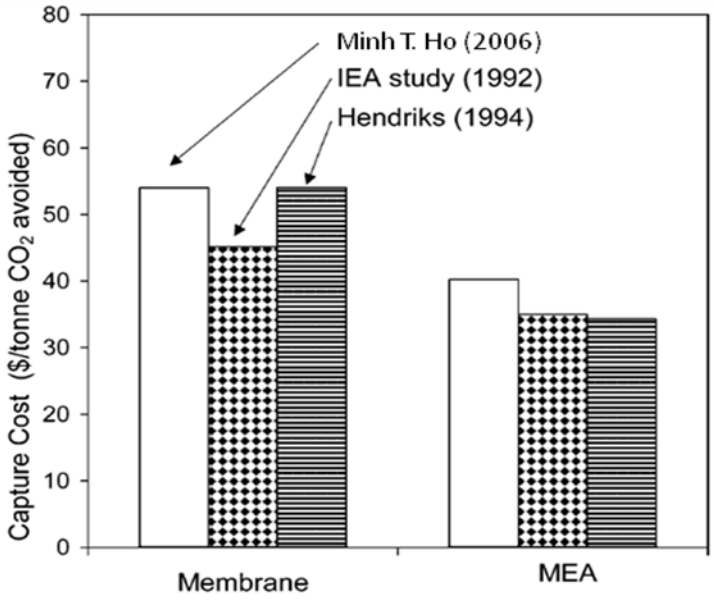

Figure 9:Comparison of CO2 capture costs for gas separation membranes and MEA [2.14]

2.3.3 Absorption vs. Membrane

The cost for CO_2 capture with absorption method is lower than that of membrane method. The need of a compressor and its large energy consumption increases the capturing cost of the membrane method. The total costs are higher than the absorption method. The cost for additional purification of CO_2 product is also responsible for the higher capture cost. With one membrane, high flow rate of the stream can result in a lower purity of the CO_2 product. Therefore, in this case, a second membrane is needed to further purify the product stream to transport it to the storage site. In addition, because the smaller volume of more purified CO_2 product from the absorption method costs less for sequestration, the membrane methods becomes more costly. In conclusion, the current membrane method is not competitive enough considering the higher capture cost unless the selectivity of the membrane increases largely without any permeability decrease.

2.4 CO_2 Emission and Power Plants in Pennsylvania

Pennsylvania is one of the most coal-producing states in the U.S. (the fourth most coal-producing state in 2006, 5.7% of the U.S. total). The abundance of coal makes possible that Pennsylvania generates most of its electricity from coal-fired power plants. There were 78 coal-fired power plants in Pennsylvania in 2005, with the total capacity of 20,475 MW, which accounted for 41.5% of the total electricity generating capacity of the state. This also made Pennsylvania the

fourth among the states which produce energy from coal. In that year, each person in the state produced 21.84 tons of CO_2. In 2006, the CO_2 emission of Pennsylvania was 117 million tons of which coal-fired power plants responsible for 43.1% [2.19]. Pennsylvania became the third CO_2-emitting state in 2007 with the 128 million tons of CO_2 emitted [2.20]. Therefore, mitigating CO_2 is an urgent issue in Pennsylvania which requires an immediate action.

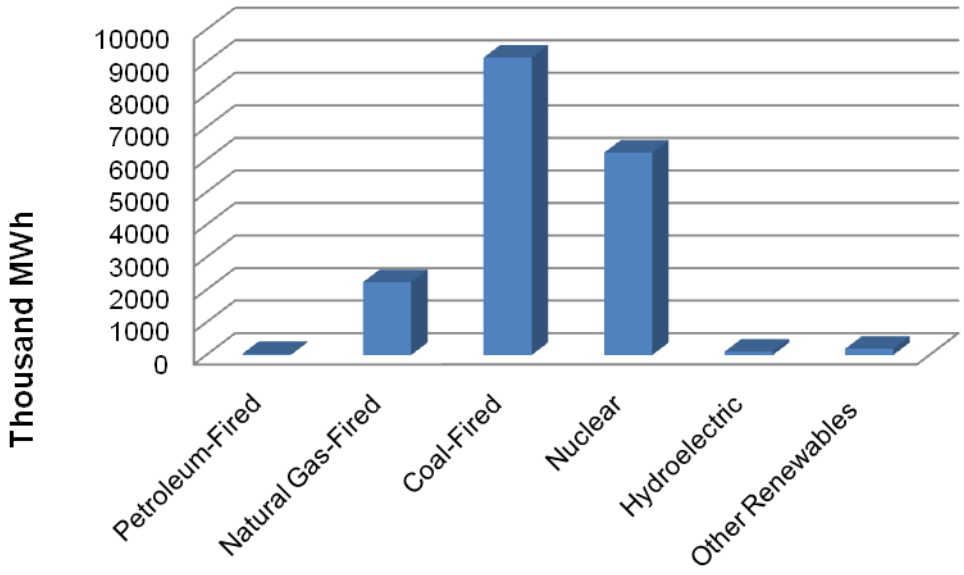

Figure 10: Net electricity generation of PA in AUG 2008 (EIA, Jan 2009)

In this work, a coal-fired power plant with a capacity of 600 MW in Indiana region is used to investigate the effect of CO_2 capture process application. The aimed CO_2 capture amount is 2.76E9 lb CO_2/year which is 1% of the total Pennsylvania annual CO_2 emission from the power industry. The aimed CO_2 capture amount was determined based on the regional greenhouse gas initiative(RGGI) in which the seven Northeastern states not including Pennsylvania are involved to reduce CO_2 emission from power industry by 10% over ten years. However, for the proper demonstration of the CO_2 capture process in the coal-fired power plants in Pennsylvania, a certain amount time is needed to test stability of the process, study effects on power plant efficiency and electricity production cost, and figure out CO_2 capture cost. Thus, in this project, the analysis for a power plant to reduce 1% of the state's annual CO_2 emission from the power industry and to keep the CO_2 emission the same for ten years was performed. This reduction can be achieved through reducing the reference power plant's CO_2 emission by 42%.

2.5 Process Design

2.5.1 Process Description

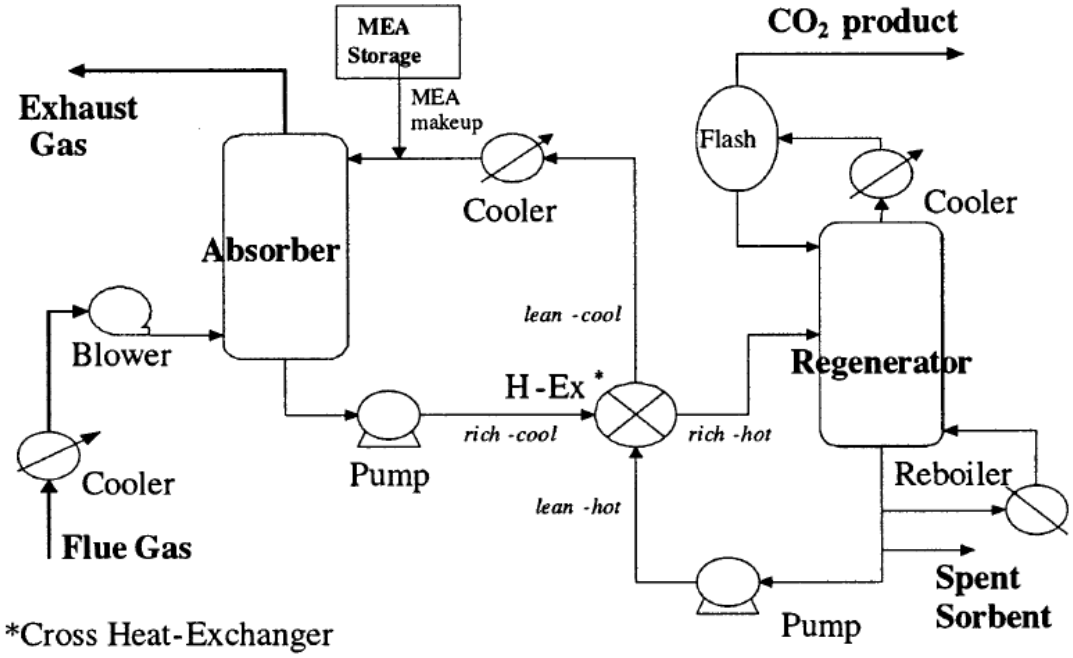

Figure 11: Flow sheet for CO_2 capture from flue gases using amine-based system [2.2]

Flue gas enters a cooler where it is cooled by a circulating-water stream. The gas is compressed in a blower to reduce the effect of pressure drop in the absorber. The gas flows into the absorber and then the absorbent captures CO_2 in the flue gas by chemical reaction. The CO_2-lean gas is washed in the wash section of the absorber, where entrained absorbent and water are removed and returned to the absorber. The cleaned gas flow out to the atmosphere. The CO_2 rich solution from absorber is pumped to the heat exchanger where hot CO_2-lean solution and cool CO_2-rich solution exchange heat.

In the solvent regeneration process, the CO_2-rich solution is heated in a reboiler by low-pressure steam. From the heating, absorbent and water are vaporized. The water and absorbent vapors go into the regenerator. The vapors are condensed as moving up in the regenerator while releasing CO_2 and heating the solution which flows downwards. CO_2 and some vapor flow into the reflux condenser where CO_2 is cooled and water is condensed. This condensed water goes back to the regenerator.

The CO_2-lean solution coming out of the reboiler is cooled in the heat exchanger. Then, the solution is pumped and cooled more before reentering the regenerator.

2.5.2 Types of Absorbent

Absorbents are classified by considering their reactivity to CO_2. Alkanolamines are most widely used absorbents. They are used in forms of water solution. There are three classes of alkanolamines; primary, secondary and tertiary amines. The degree of substitution of the hydrogen on the nitrogen atom is the criterion for the classification of alkanolamines; two H atoms on nitrogen (primary), one H atom (secondary), no H atom (tertiary). Monoethanolamine (MEA) is an example of primary amines, and is the most reactive absorbent to CO_2 among the amines. Diethanolamine (DEA) is an example of secondary amines. Triethanolamine (TEA) is a tertiary amine, which reacts with CO_2 only if the partial pressure of CO_2 is higher than atmospheric pressure. This makes tertiary amines not attractive for capturing CO_2 from the flue gas of a coal-fired power plant.

<Reactions for MEA, DEA> [2.17][2.18]

(1) Bicarbonate formation : $CO_2 + RNH_{X+1} + H_2O \leftrightarrow RNH_{X+2}^{+} + HCO_3^{-}$

(2) Carbamate formation : $CO_2 + 2RNH_{X+1} \leftrightarrow RNH_{X+2}^{+} + RNH_XCOO^{-}$

(3) Carbamate reversion : $CO_2 + RNH_XCOO^{-} + 2H_2O \leftrightarrow RNH_{X+2}^{+} + 2HCO_3^{-}$

FOR MEA : R = $-CH_2CH_2OH$; X=1

FOR DEA : R = $(-CH_2CH_2OH)_2$; X=0

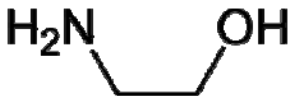

<MEA>

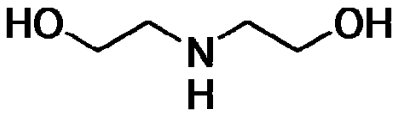

<DEA>

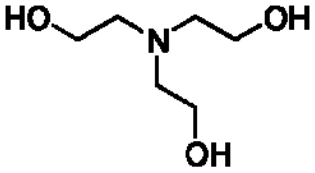

<TEA>

2.6 Calculation for Efficiency and Power Loss

The CO_2 capturing system can be easily implemented without significant changes to power plants. The flue gas goes into absorption unit which requires solvent regeneration later in the process. Low-pressure steam extracted from the power plant steam cycle is used to supply the heat for the regeneration process. This regeneration process significantly decreases the efficiency of the power plant. The energy for compressing the flue gas and the captured CO_2, and solvent pumping can also cause the efficiency drop.

2.6.1 Flue Gas Compression and Solvent Pumping (P_{scrub})

There is a power demand for moving the flue gas and the solvent (P_{scrub}) because of the pressure drop during the capture process. For conventional coal-fired power plant with a capacity of 600MWe, the energy consumption of pump and blower is 5.7 MWe (for mono-ethanolamine) and 6.7 MWe (for diethanolamine) [2.17]

2.6.2 Steam Extraction (P_{extr})

The heat for solvent regeneration comes from low-pressure steam generated in the reboiler of steam cycle. The reboiler increases the temperature of the supplied water to produce steam, which is used to provide enough thermal energy needed for solvent regeneration. The amount of steam needed to capture one lb of CO_2 (lb steam/lb CO_2) can be calculated from

$$m_{steam} = \frac{Q_{CO_2}}{(H_{LP}^{S} - H_{reb}^{W})}$$

Where Q_{CO_2} is the heat required for capture one lb CO_2 (Btu/lb CO2), H_{LP}^{S} is the enthalpy of the steam (Btu/lb steam), and H_{reb}^{W} is the enthalpy of the water supplied to the reboiler (Btu/lb water).The power loss from steam extraction for one lb of CO_2 (Btu/lb CO_2) can be also calculated from

$$P_{extr} = m_{steam} \times (H_{LP}^{S} - H_{1}^{S}) \times \eta_{gen}$$

Where H_{1}^{S} is the enthalpy of the water leaving the water condenser in the solvent regenerator (Btu/lb steam), η_{gen} is the efficiency of the generator (%).

2.6.3 CO_2 Compression (P_{comp})

The captured CO_2 comes out at 35 psia that should be pressurized to 1500 psia to be transported to the storage site. This compression can be done successfully by alternating cooling and compression CO_2 flow. A four-step process appears to be a good compression method. According to the pressure and enthalpy diagram of CO_2, a four-step isentropic compression requires 132 Btu/lb CO_2. With an isentropic efficiency of 85%, the compression process requires 155 Btu/lb CO_2 [2.17]

2.6.4 Loss of Plant Efficiency (η_{loss})

The loss of plant efficiency (%) can be calculated by dividing the power loss of power plant by the heating value of the fuel.

$$\eta_{loss} = \frac{\alpha_{CO_2} \times P_{loss}}{Q_{fuel}}$$

Where,

$$P_{loss} = P_{extr} + P_{scrub} + P_{comp}$$

α_{CO2} is the absorption efficiency of CO_2 recovery(%), Q_{fuel} is heating value of fuel per lb CO_2 produced (Btu/lb CO_2)

2.6.5 Result

The calculation for plant performance is done for two different solvents (MEA, DEA). The values for the calculation are taken from an existing coal-fired power plant with a similar capacity of our referred power plant. The result shows that the efficiency loss for the CO_2 capture using MEA is higher than that of using DEA. This is largely because the enthalpy change of the reaction between CO_2 and solvent is bigger in MEA absorption, which leads to the fact that the heat required for solvent regeneration is more in MEA absorption. In other words, MEA absorption consumes more steam than DEA absorption for solvent regeneration.

Table 3: Key values for the calculation of the power loss by CO2 recover for the Amer-8 power plant [2.17]

Q_{fuel}	4567 [Btu/lb CO_2]
α_{CO_2}	42 [%]
H_1^S	988 [Btu/lb steam]
η_{gen}	99 [%]

Table 4: Results as calculated for two different cases

		MEA	DEA
Q_{CO_2}	[Btu/lb CO2] [2.17]	1590	1435
H_{LP}^{S}	[Btu/lb steam] [2.17]	1235	1213
H_{reb}^{W}	[Btu/lb water] [2.17]	202	182
P_{loss}	[Btu/lb CO2]	552	490
η_{loss}	[%]	5.3	4.5

2.7 Economical Analysis

Table 5: Economic analysis assumptions

Project life(years)	10
Operating hours(hour/year)	6000
Operation and maintenance cost(% of capital cost)	3
Interest rate (%)	5
Spent solvent making up ($/ton CO2 captured)	4
SO_X, NO_X in flue gas (ppm)	70
Coal price ($/ton)	48

2.7.1 Capital Cost

The capital cost for a power plant with CO_2 capture process has three parts: power plant cost, capture process cost, and compressor cost. For power plant, building a 600MW power plant costs 690 million USD, including interest rate. For capture process, the Econamine FG process is applied. The cost for the capture process also includes the cost for flue gas cooler, flue gas blower, heat exchanger, and solvent regenerator. This cost tends to increase as the concentration of CO_2 in flue gas decreases because a lower concentration of CO_2 needs a bigger absorber. In this work, the CO_2 amount in the flue gas is assumed to be 13%. The cost for the absorber accounts for 40% of total capital cost for the capture process, and the solvent regenerator is second most expensive, which takes up to 20% of the capital cost. In total, 182 million USD is needed for the chemical absorption unit. For CO_2 compression, a compressor with a capacity of 500 ton CO_2/hour is applied in this work. The capital cost for the unit is 25 million USD. [2.11][2.17].

2.7.2 Annualized Cost

To calculate electricity production cost and CO_2 capture cost, an annualized cost for the process needs to be considered. Annual charge for a 600MW power plant with capture process is 68 million USD, which includes labor cost, taxes, distribution, marketing, R&D cost, and so on. Coal feedstock consumes 63 million USD a year. Operation and maintenance costs (O&M) for power plant with CO_2 capture process are assumed to be 29 million USD a year, which is 3% of the total capital cost. Spent solvent making up is responsible for almost 30% of the O&M cost. An incinerator can burn the spent solvent and the gas coming out of the incinerator is purified before released. The cost for disposing solvent costs 100 USD per ton of solvent. [2.2][2.11][2.17]

2.7.3 CO_2 Capture Cost and Electricity Production Cost

Table 6 shows an overview of CO_2 capture cost using MEA solvent. The electricity production costs were calculated through dividing annualized cost by net electricity production (kWh/year). The CO_2 capture using chemical absorption increased the electricity production cost by 46%. In addition, the technique costs 48.6 USD per ton CO_2 avoided. For CO_2 capture using DEA, bigger equipment is needed because the solvent reacts with CO_2 slower than MEA; therefore, the size of heat exchanger, circulation rate, and the size absorber should be increased. However, we are not able to figure out the degree of the equipment size increase so that we cannot perform economical analysis [2.17].

Table 6: Overview of CO_2 capture cost using MEA in 600MW coal-fired power plant

Capital cost(million USD)		
	Reference plant Construction	690
	Chemical absorption unit	182
	CO_2 compressor	25
	Interest during construction and land site	59
Total		957
Annualized cost(million USD/year)		
	Capital charges for reference plant	49
	Capital charges for CO_2 capture components	19
	Coal feedstock	63
	Operation and maintenance cost for reference plant	22
	Operation and maintenance cost for CO_2capture process	9
Total		162
Net power production(MW)		
	Reference plant	600
	Power plant with CO_2 capture	568
Electricity production cost(cent/kWh)		
	Reference plant	3.7
	Power plant with CO_2 capture	5.4
Specific CO_2 emission (lb/kWh)		
	Reference plant	1.8
	Power plant with CO_2 capture	1.1
CO_2 capture cost (USD/ton CO_2 avoided)		48.6

Chapter 3

Sequestration of CO_2

3.1 Sequestration

Sequestration is the process of isolating CO_2 from the environment. It is one of the most promising ways for controlling the concentration of CO_2 in the atmosphere [3.3]. Sequestration can be classified into two broad categories: Geologic sequestration and Terrestrial sequestration. Geologic sequestration involves the capture and disposal of anthropogenic CO_2 in geologic sites. Various geologic sites identified so far includes producing or abandoned oil and natural gas reservoirs, un-mineable coal seams, deep saline aquifers, deep ocean injection. During the storage of the CO_2, the gas stream is compressed to its critical condition so that the maximum amount of gas can be injected in the geologic sites [3.5].

Net removal of CO_2 from the atmosphere of prevention of CO_2 net emission from the terrestrial into the atmosphere is termed as Terrestrial sequestration. The research can be focused onto two tasks: protecting the eco-system that can store carbon and enhance the intake of carbon in the carbon cycle and secondly, manipulation of ecosystems to increase the carbon sequestration beyond the current level [3.4]. These tasks can be achieved by promoting forestation. This chapter is focused on studying carbon dioxide sequestration in depleted oil/gas reservoirs and injecting CO_2 in deep saline aquifers.

3.2 CO_2 sequestration in depleted oil/gas reservoirs

CO_2 sequestration in depleted oil/gas reservoirs can be considered as a possible long term solution as the estimated sequestration capacity is reported to be around 140 Giga tones of carbon in gas reservoirs around the world [3.6]. The first large scale underground disposal of CO_2 was carried by Norwegian state oil company, Statoil, in North Sea. Under the same study carried by Halloway et. al. (1995), it was suggested that 0.95 giga tone of carbon dioxide will need to be sequestered in North Sea [3.8]. Based on the assumptions, the storage capacity of the offshore gas reservoir was calculated to be 13.3 giga tones and the onshore gas storage capacity was estimated at 13.1 giga tones. The storage capacity of the offshore oil reservoir was calculated as 5.9 giga tones and the onshore oil reservoir was reported as 0.22 giga tones. In order to calculate the storage capacity of the reservoir it is assumed that the space vacated by the HC[†] will be completely occupied by carbon dioxide [3.9]. The storage capacity calculated by this method is also known as theoretical sequestration capacity.

[†] Hydro-Carbon

The other terms useful for the study are effective and practical sequestration capacity. "The effective capacity is the more realistic estimate obtained after water invasion, displacement, gravity, heterogeneity and water-saturation effects have been taken into account. Practical capacity is the sequestration capacity after consideration of technological limitations, safety, CO_2 sources and reservoir distributions, and current infrastructure, regulatory and economic factors" [Bachu S. (2004)]. In the end, all the issues and factors relating to CO_2 capture, delivery and sequestration contribute to a reduction in the real capacity for CO_2 sequestration in hydrocarbon reservoirs [Bachu S. (2004)].

It has also been reported that gas reservoirs can store significantly more CO_2 than a depleted oil reservoirs as gas reservoirs have about 65% recovery of GIIP[‡] which is nearly twice the recovery observed in oil reservoirs with 35% of OIIP[§] [3.7]. However, sequestration of CO_2 has not been carried and well understood in natural gas reservoirs. In order to understand the mechanism of CO_2 injection for sequestration, phase behavior of CO_2, pure methane and their mixture must be studied. In the early stages of the process, three different zones of gases are observed that consists of pure natural gas, mixture of natural gas and carbon dioxide, and pure carbon dioxide. With time, these zones mix together to form a homogeneous mixture of natural gas and carbon dioxide [3.6].

Phase behavior of the fluids is important to understand the compressibility factor of the gas phase and the amount of fluids present in the reservoir at the reservoir and surface conditions. These properties are calculated as a function of pressure, temperature and the composition of the gas. The critical temperature and pressure conditions for CO_2 are 31˚C (88˚F) and 7.38 MPA (1070 psia). Whereas, reservoir pressure and temperatures are encountered between a range of 500-3000 psia and 68˚– 174˚ F and if the phase behavior of carbon dioxide is studied then it can be seen that CO_2 in most of the reservoir will fall in the critical region for these values as can be seen in the Figure 12.
Reservoir pressure and temperature is a function of its depth from the surface given by equations 1 and 2. In this equation pressure is measured in 'psia', temperature is measured in '°F' and depth is measured in feet.

$$P = 14.7 + 0.4538 * d \quad (1)$$

$$T = 61 + 0.007 * d \quad (2)$$

From the above expression we can see that a reservoir at a depth of 800 m (2600 ft) or more will be more effective in CO_2 storage or we can see that shallow reservoirs do not provide sufficient

‡ Gas Initially-In-Place
§ Oil Initially-In-Place

storage as the gas will remain in the gaseous phase in the reservoirs. Therefore, it will not be efficient to store gas in those reservoirs as compared with the deep reservoirs where CO_2 attains the supercritical stage and has high molar density. Moreover, Supercritical CO_2 has low surface tension which allows it to diffuse more easily on surfaces with regular & irregular geometry, and through pore spaces and hence it becomes easier to inject CO_2 in the reservoir.

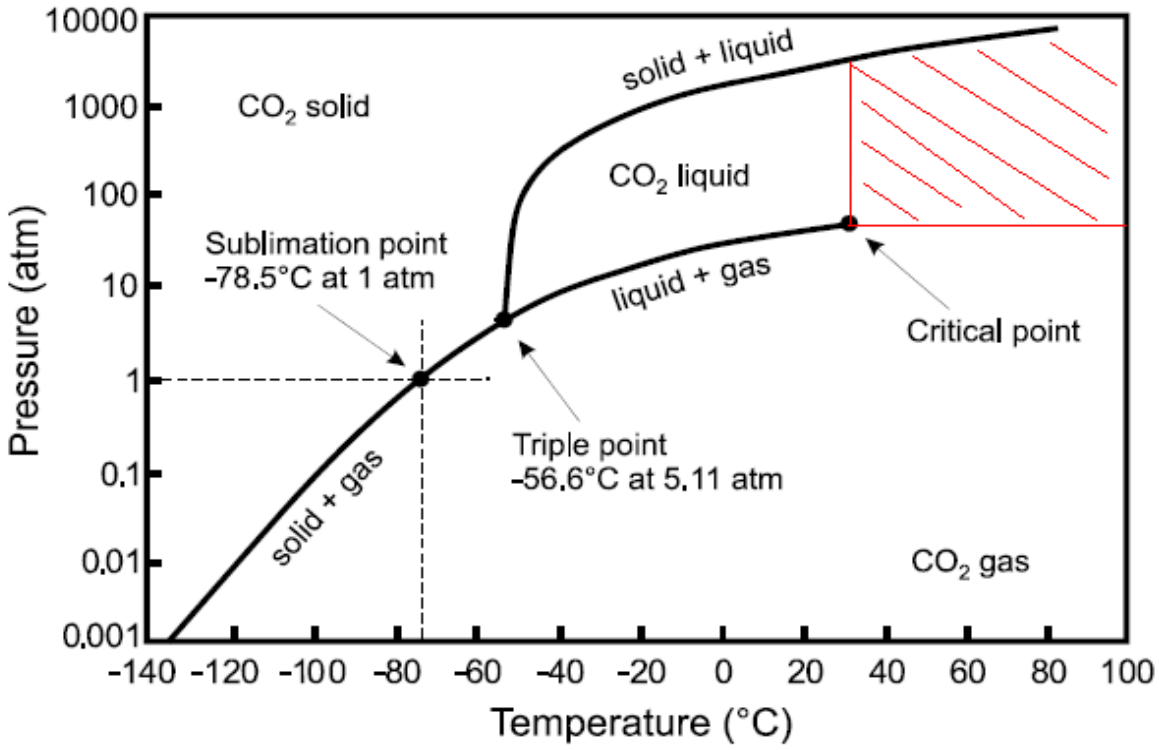

Figure 12: Phase behavior of Carbon Dioxide (Source: General Chemistry, Chemical of the Week)

3.2.1 Important parameters and CO_2 Sequestration calculations

It is important to find out the important variables that control the sequestration process. Some of the identified variables are volume of the reservoir, porosity of the reservoir, horizontal and vertical permeability of the reservoir, injectivity of the wells, pressure of the reservoir, reservoir integrity, production history of the reservoir, water chemistry, the nature of the cap-rock or reservoir seal, source of carbon dioxide and infrastructure available for transportation of the gas. Amount of CO_2 that can be sequestered in the reservoir can be calculated as:

$$Q_{CO_2} = \rho_{CO_2} * \emptyset * A * H * (1 - S_w)/2200 \quad (3)$$

Where, 'Q_{CO2}' is the theoretical sequestration capacity in 'metric tons', 'ρ_{CO2}' is the density of CO_2 at the reservoir conditions in 'lbs/acre-ft', 'ϕ' is the porosity of the reservoir, 'A' is the area of the reservoir in acres, 'H' is the thickness of the geological sequestration unit in 'ft'and 'S_w' is the water saturation present in the reservoir. This model of calculation assumes that all the values are average estimates of the reservoir, the volume left by HCs can be fully occupied by CO_2. This model also assumes that no diffusion of CO_2 occurs in the pores of the reservoir, geo-chemical reactions of CO_2 with the reservoir rock and compositional effects of CO_2 injection are not observed.

3.2.2 Technical Challenges for CO_2 Sequestration

There are various technological challenges that need to be addressed before implementing geological sequestration of carbon dioxide. Challenges include calculating the optimum amount of CO_2 that can be stored in the geological site. This factor will depend upon understanding the chemistry of the fluids at reservoir conditions, heterogeneous behavior of the reservoir, strength of the cap-rock to hold the gas, geology of the reservoir present near to the one in question, infrastructure availability, carbon dioxide source and the economical considerations [3.9]. Other technical challenges include in predicting the probability of migration of CO_2 from the location of storing it, the risks associated with the migration and monitoring of the leakage in advance [3.2].

Since CO_2 is lighter than the water contained in the reservoir rock, there is a tendency for the fluid to escape through the migration path already built by HCs. The containment of CO_2 will depend upon the structural seals of the reservoir holding a large gas cap of CO_2. The leakage of the fluid can be reduced by minimizing the mass of CO_2 in the gas cap. CO_2 is a non wetting phase in the reservoir and thus experience larger capillary forces. These forces are more than the buoyancy forces which helps in storing it in the reservoir [3.2]. But if the buoyancy force somehow overcomes the capillary forces then there is a good probability of leak. However, this will depend upon the density of CO_2 in the reservoir.
Also, it has been commonly believed that the sealing capacity of the cap rock for a hydrocarbon-water system is sufficient to prevent the injected CO_2 from leaking into the atmosphere or the upper formations [3.10]. However, it has been found that the sealing capacity of the CO2-water system is considerably reduced as the interfacial tension of CO_2-water system is much lower than the interfacial tension of the hydrocarbon-water system.
Sealing capacity is a measure of the breakthrough pressure which is defined as the differential pressure across the cap rock [3.10]. This differential pressure just exceeds the capillary pressure of the interconnected pores, therefore, it can be inferred that capillary pressure determines the

breakthrough pressure of the cap rock. Capillary pressure of the interconnected pore channel depends upon the interfacial tension as shown by the Equation 4

$$P_c = \frac{2\sigma}{r_p}.\cos\theta \qquad (4)$$

Where, σ is the interfacial tension between the non-wetting (gas or oil) and the wetting phase (water), r_p is the radius of the pore throat and θ is the contact angle. Interfacial tension for n-alkane-water system at 10 Mpa and 25˚C is 49 mN/m, whereas for CO_2-water system at the 10 Mpa and 40˚C is 16 mN/m. In order to inject CO_2 in the oil/gas reservoir without leaking it back in the atmosphere, interfacial tension should be considered and the breakthrough pressure of the cap rock must be calculated.

There is still a good chance of leakage because of factors like faults reaching the earth's surface and human activities like buildings, homes, extraction of sub-surface minerals etc. In these scenarios, a study must be carried to determine how fast CO_2 will move along the leak. According to Bryant et. al. (2007), the rising fluid dissolves in the brine and thus the upward movement of carbon dioxide is reduced but the density and solubility of carbon dioxide reduces with the reducing pressure. However, the capillary pressure is increased because of the decreased density. Therefore, CO2 moves laterally and the effect of the leak can be spread over a wider area. In order to understand and learn more about the leakage, pre-monitoring of the leak must be done in advance.

3.2.3 Engineering Approach for CO_2 sequestration in depleted oil/gas reservoir

In order to carry out the study in a depleted oil/gas reservoir, a hypothetical reservoir is assumed in State College (PA) area which has properties similar to a reservoir in New Mexico. The problem is studied using a commercially available reservoir simulator (CMG-GEM) and the engineering analysis and preparation of the reservoir for the simulator is discussed in Appendix A. In order to calculate a rough estimate of the sequestration capacity of CO_2 in the reservoir the available pore space is calculated as shown in Table 7.

Table 7: Pore volume of each layer

Layer	# of Active reservoir blocks	Δx	Δy	h	ϕ	Pore Volume (ft^3)
1	972	200	200	16	0.1373	$1.922*10^8$
3	972	200	200	12	0.1622	$1.703*10^8$
5	972	200	200	6	0.075	$0.394*10^8$
7	972	200	200	6	0.075	$0.394*10^8$

The total pore volume for CO_2 from the table is $4.413*10^8$ ft^3 and the amount of CO_2 that can be sequestered in the reservoir is calculated using volume formation factor (FVF) an estimated value for FVF is taken as 0.0048 [Xu. J. et al. (2007)]. Therefore, the total theoretical volume for CO_2 is $9.194*10^{10} ft^3$.

In this study CO_2 captured in a power generation plant in Indiana region will be sequestered. The capturing capacity of the plant is $2.79*10^9$ lbs/year which can be converted into field units by the following equations.

$$1\ lbs\ of\ CO_2 = \frac{1}{44}\ lb\ mol\ of\ CO_2 \quad (5)$$

$$1\ lb\ mol\ of\ CO_2 = 379.1\ SCF\ (sft^3)\ of\ CO_2 \quad (6)$$

From the calculations, it is found that $2.404*10^{10}$ ft^3 of CO_2 is captured annually in the plant. CO2 can be sequestered in the reservoir in two ways: first when the whole of the captured amount is sequestered in the reservoir or secondly, a fraction of the amount is sequestered. In the first approach, according to the calculations the reservoir can store the entire amount of CO_2 captured in the power plant for nearly 4 years where $1.38*10^7$ ft^3 of CO_2 will be injected daily at each of the 5 wells (or a total of $6.9*10^7$ ft^3/day in the reservoir). When the whole amount of the captured CO_2 was injected into the reservoir then the wells crossed the threshold limit of the cap rock pressure which is set at 7000 psia as shown in Figure 13. From the above calculations and observation, injection of the whole amount of captured CO2 in the reservoir is not feasible. Therefore, a fraction of the amount of CO_2 captured will be injected and stored in the reservoir.

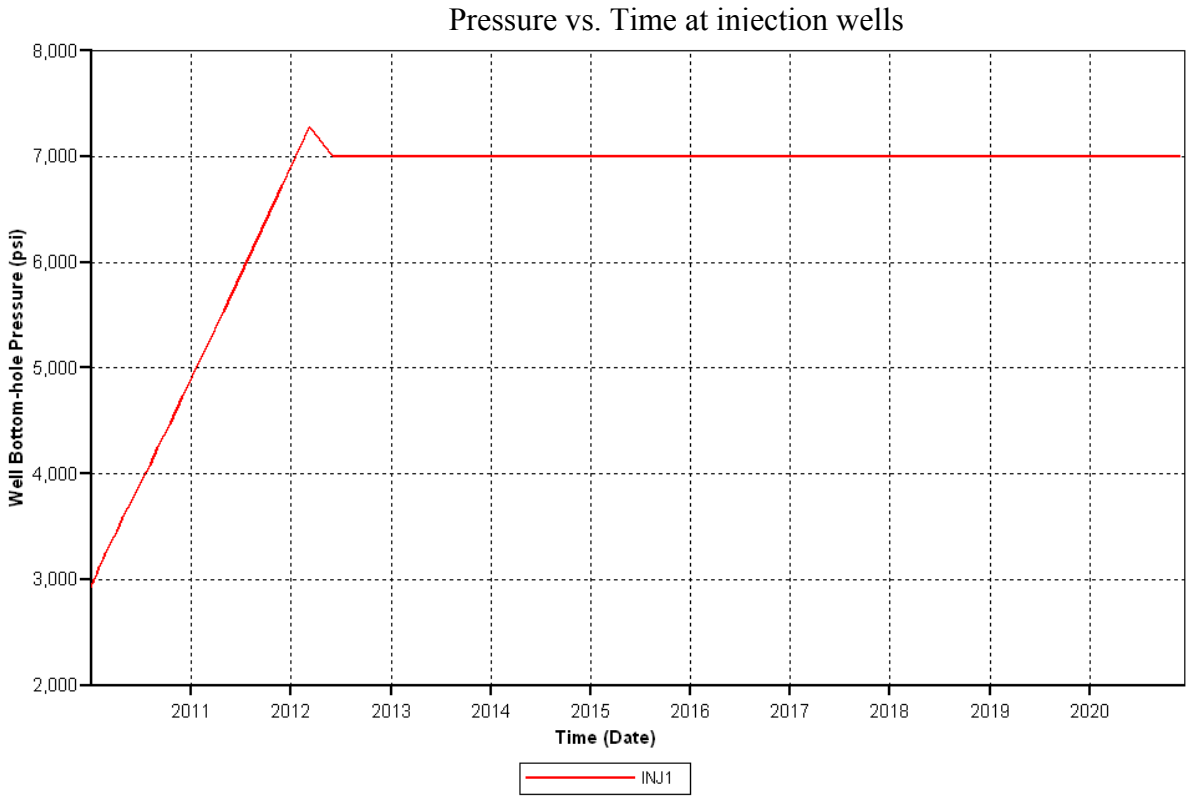

Figure 13:Pressure changes at an injection well with time

The study is carried for 10 years and the amount of CO2 is calculated which will not break the sealing capacity of the rocks or abandoned wells. In this study, CO_2 will be injected in the reservoir at a total injection rate of $2.519*10^7$ ft^3/day ($1.067*10^9$ lbs yearly), and there are 5 wells in the field which are used for injection at an injection rate of $5.038*10^6$ ft^3/day. Pressure changes at the well are observed at this injection rate which is found to stay under the threshold limit as shown in Figure 14. Movement of Carbon Dioxide is also studied in the simulation and the global mole fraction of CO_2 in the reservoir at different times is shown in Figure 15.

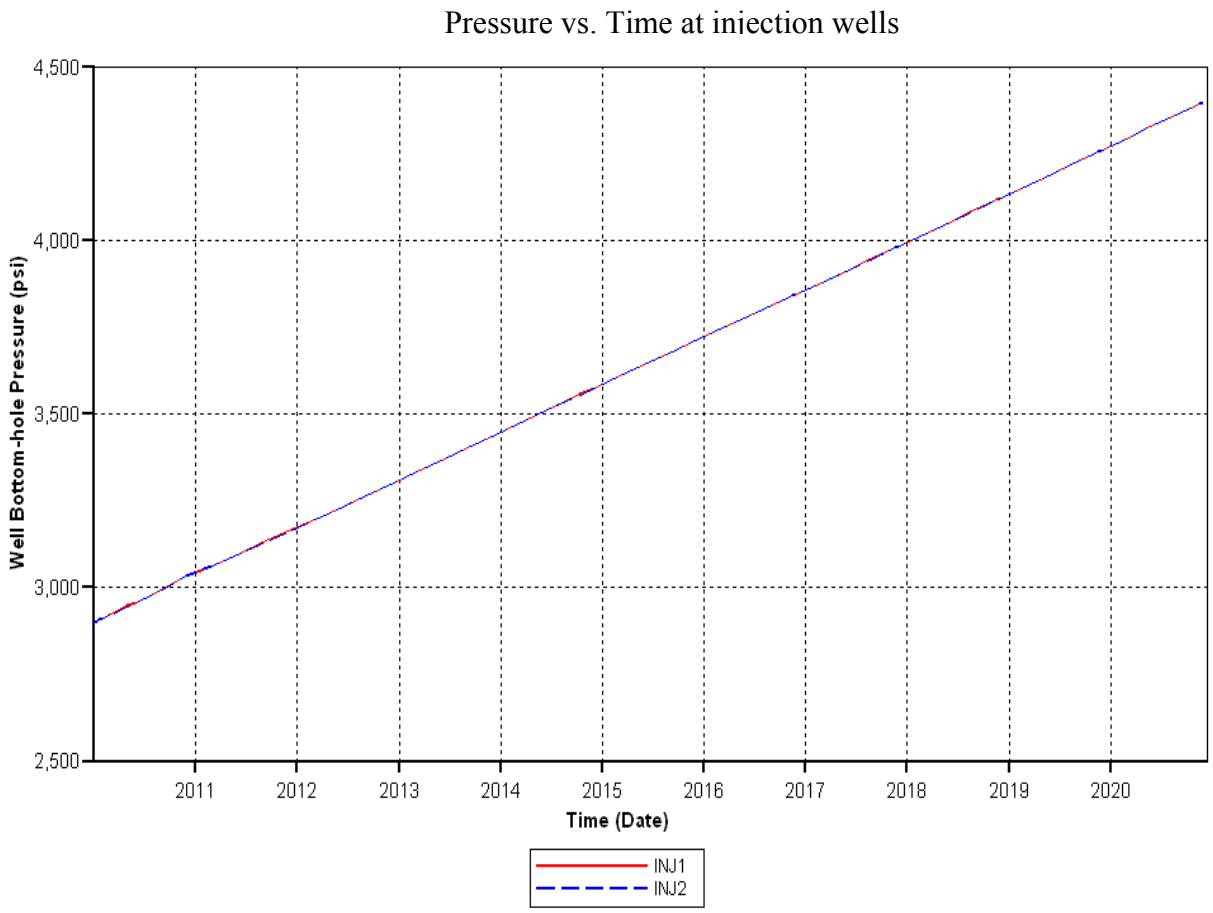

Figure 14: Pressure changes at an injection well with time at optimized injection rate

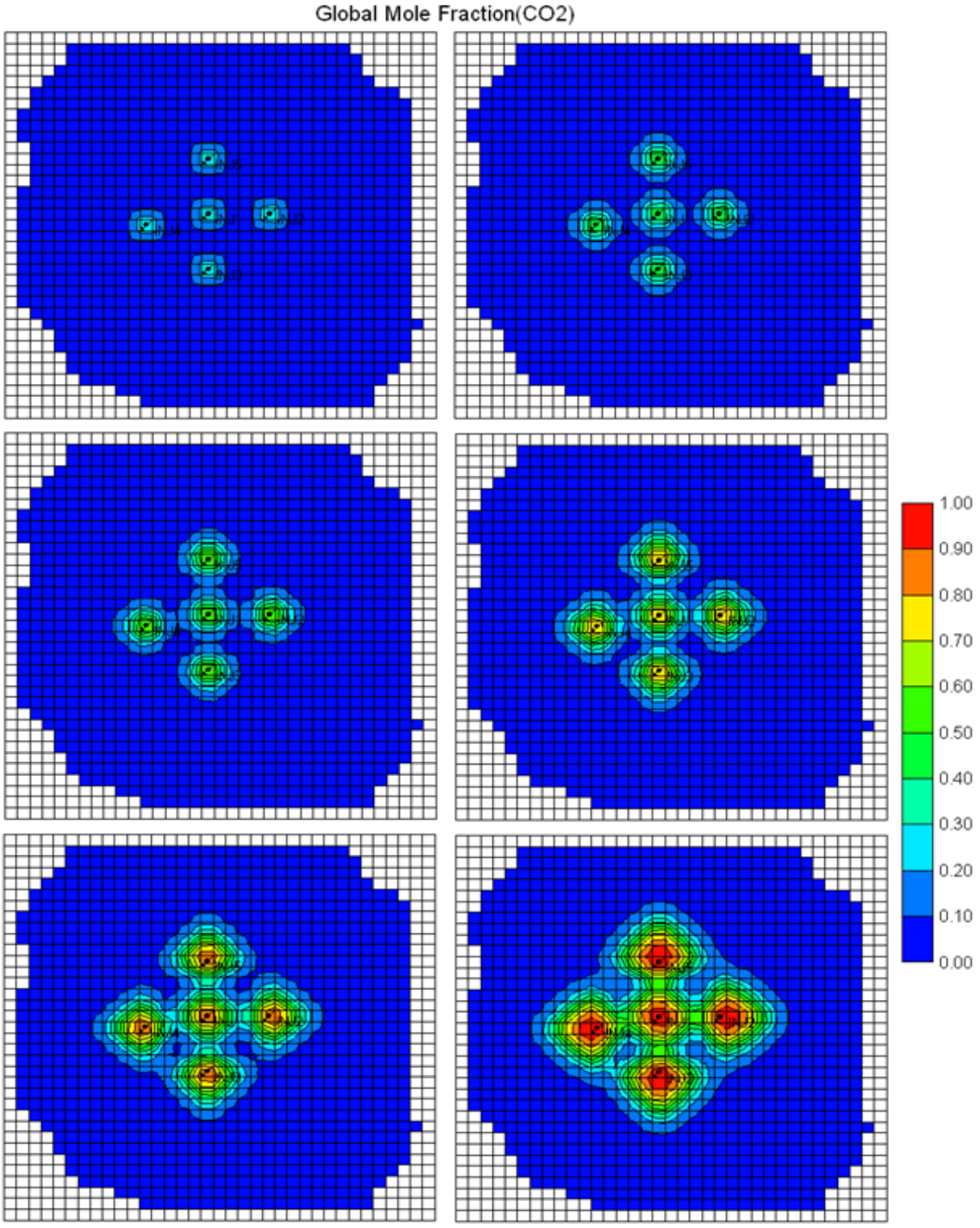

Figure 15: Movement of CO2 in the reservoir

In the same reservoir leakage effects were also studied where one of the five wells was assumed to be an abandoned well and was not used for injection. CO_2 was injected from the rest of the 4 wells at the same abovementioned injection rate. A pressure gradient of 20 psia was assumed at one of the well and a part of the gas injected from the rest of the four wells was leaking from the well. It was also assumed that the leakage was not stopped during the course of the study from the well and a total amount of leakage was calculated from the well from the plot shown in Figure 16. A total of $5*10^6$ ft^3 of CO_2 leaks from the reservoir which is $5.43*10^{-3}$ percent of the total amount of CO_2 sequestered in the reservoir. Movement of CO_2 was also studied in the reservoir and the global mole fraction of CO_2 at different times is shown in Figure 17. This figure also shows the dampened CO_2 movement profile around the leakage well where lower pressure was also observed.

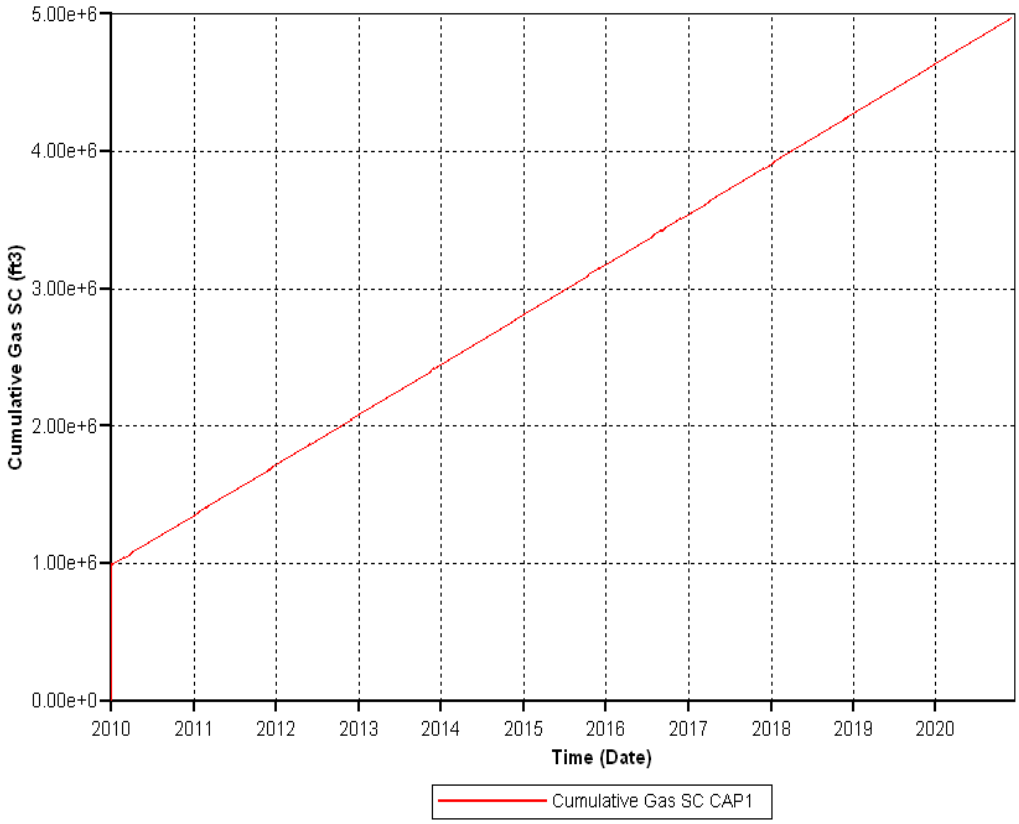

Figure 16: Cumulative amount of CO2 leakage from the well

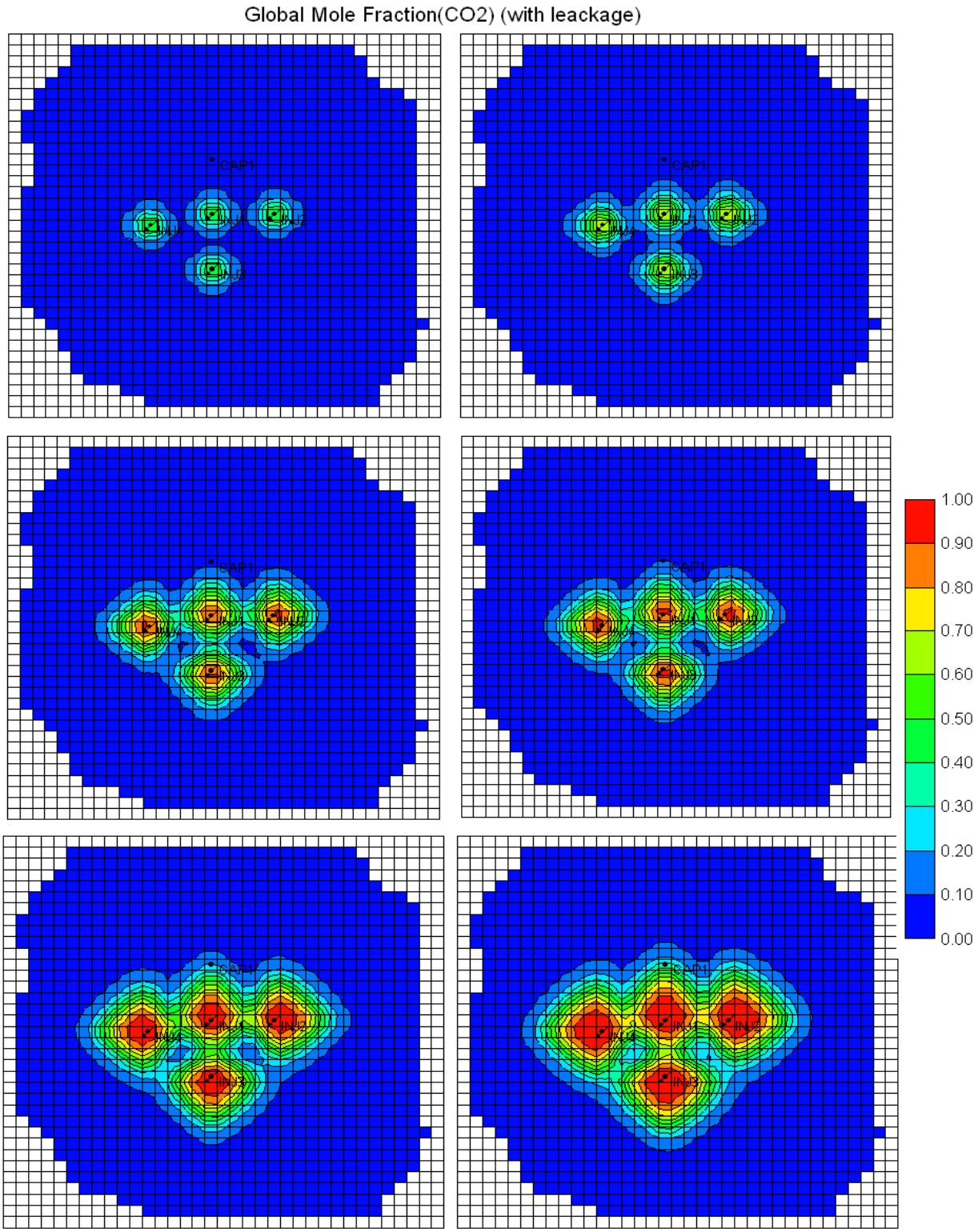

Figure 17: Movement of CO2 in the reservoir when leakage in one well is accounted

3.2.4 Economical analysis of CO_2 Sequestration

The economical analysis includes the capital cost and operating cost for the sequestration process. The capital cost can be broken down into building the facility for CO_2 injection at the sites, pipelines infrastructure and the separation equipment for CO_2 from natural gas. Sometimes, the cost of separation is excluded from the sequestration cost analysis because the natural gas has to be processed before selling regardless of sequestering CO_2 [3.5]. The cost of building pipe line will depend upon the distance and the requirements of compression stations in between the separation and the sequestration site. The cost of compression is also a function of the rate of CO_2. Figure 18 shows sequestration capital cost as a function of CO_2 flow rate and the distance between source and sink.

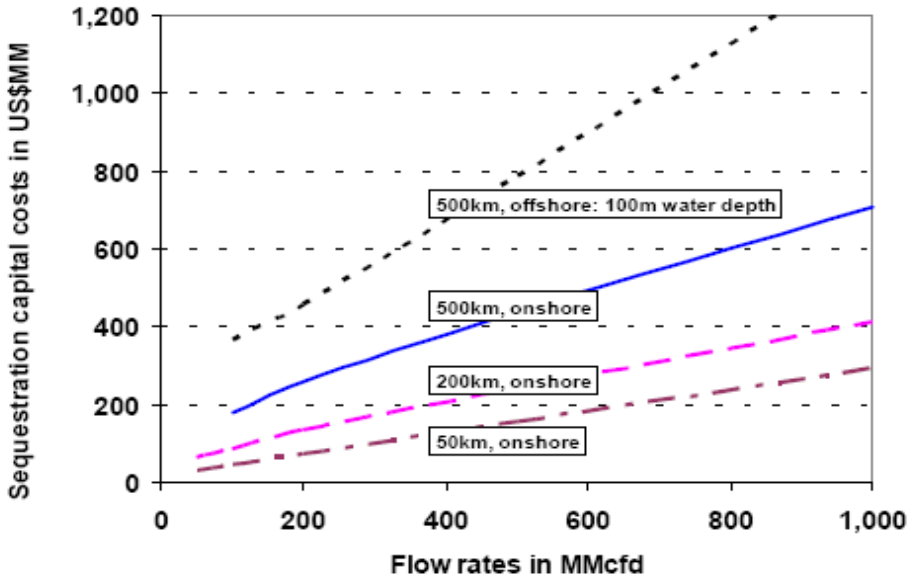

Figure 18 Sequestration Capital costs against CO_2 flow rates and distance [3.5]

Sequestration cost will also depend upon the type of reservoi. Different reservoirs have different permeability and thus injectivity. A similar analysis is shown by Nguyen et. al.(2003) and is shown in Figure 19 which shows the sequestration cost in different permeable systems and sequestered at different flow rates. In developing this relationship a constant distance of 500 kilometers was assumed.

In this project, the reservoir considered for sequestration is a hypothetical reservoir in Pennsylvania which is assumed to be at a distance of 500 Km away from the capturing site. Since we already have calculated the flow rate of CO_2 to be injected in the reservoir, we can use Figure 18 to find the capital cost of installation for the process. We are injecting 250 MMcfd of CO_2, therefore, a capital cost of building pipelines and compressor stations an investment of $290 million are required.

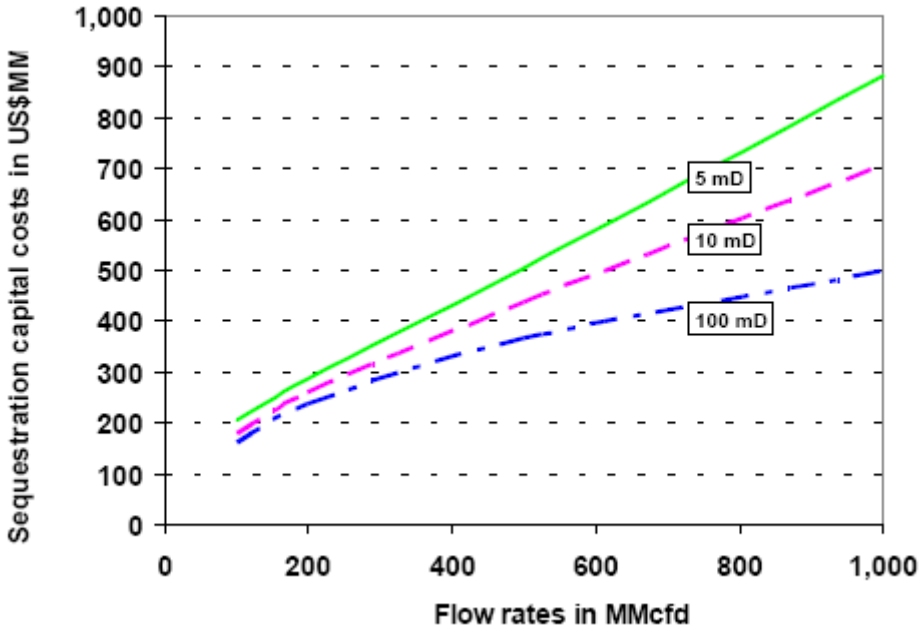

Figure 19: Sequestration capital cost against reservoir permeability [3.5]

It is also shown that the sequestration capital cost also depends upon the type of reservoir which is a function of permeability. Since, the reservoir has four permeable layers with different permeability in each zone; an arithmetic average is taken for the completion zones, which is 111 mD. Due to unavailability of the curve for this permeability the nearest curve is chosen for determining the capital cost. From the graph the, for this reservoir an initial investment of $260 million is required.

Since the capital cost required for the process by the first method is higher therefore in the economical analysis the higher value will be used. Leasing cost of the field is not assumed as this is an exhausted field. Since there is no production from the field, royalty cost of the production is absent. With these assumptions there will be only capital and operating costs. Using these values we can find the amount that should be charged to sequester CO_2 in this geological sequestration procedure. According to the equation given below, we can find the net present worth of the net daily cash flow of operation and that should be equal to the initial capital investment. Operating costs will be incorporated in the net daily cash flow.

$$\frac{P}{A} = \frac{[(1+i)^n - 1]}{i(1+i)^n}$$

In this equation, present worth is equal to the initial investment of $260 millions, and an annual interest rate of 5% is assumed (or 0.0137% daily interest rate) and since the process of sequestration is carried for 10 years, ‘n’ would be equal to 3650 days. Using the above relation

we can find the net daily cash flow to be $90526. Since, 250 MMSCF of CO_2 is being daily sequestered using this method; the net cash flow per MSCF can be calculated to be $0.4924/MSCF (or $8.485/ton of CO_2). The cost of sequestration calculated so far also includes operating cost. Assuming the operating cost to be 10% as a commonly accepted cost for operations; cost for CO_2 can be calculated as $0.4976/MSCF (or $7.714/ton of CO_2) [3.29]. Therefore, from the calculations $7.714/ ton of CO_2 should be charged in order to recover the capital cost within 10 years to make the sequestration process economically feasible.

3.3 Sequestration of CO_2 in Deep Saline Aquifers

3.3.1 Introduction

As stated in the main introduction of CO_2 sequestration, there are several options for sequestration some of which might have economical benefit such as EOR or coal-bed methane but their aim is not to permanently sequestrate it but to increase the production and the operation time. The other methods such as sequestration in ocean basins, exploited oil and gas fields and deep saline aquifers are in order to sequester it permanently and to mitigate the climate change which currently doesn't have any economical benefit in most countries. However, they started to be applied in some countries such as Norway or Canada due to some restrictions on CO_2 emission per energy resource. Besides, the others countries are thinking to apply similar laws in addition to the carbon trade which might boost the subsurface CO_2 sequestration which will make use of saline aquifers a must. [3.14]

3.3.2 Saline Aquifers

Saline aquifers do not have potable water and therefore can be used to sequester CO_2. They are covered by impermeable rocks and have high saline properties. Saline aquifers have some positive and negative attributes regarding its use as a sequestration site. The positive attributes are that they are large, abundant and widespread. Because they are abundant there is a very high possibility that there will be a saline aquifer close to the carbon source which will reduce the transportation cost. In addition, saline aquifers have a high storage capacity and might account for 20% to 500% of the projected total CO_2 emissions to 2050. This potential source is environmentally fit also as they are covered by impermeable rocks. [3.14] On the other hand, we do not have as much expertise in handling these reservoirs as we have for oil and gas fields. Therefore, a lot of research will be required to exploit the formation effectively. Moreover, they require expensive trapping methods and it is difficult to accurately estimate the storage capacity due to 4 different types of trapping effects which might occur at the same time as well [3.15]. Lastly, there are some economical and environmental concerns about it. They must be economically competitive with other options and mustn't harm the environment. Dealing with the societal fear is important, too. [3.14]

3.3.3 Required Physical Properties

As it will be discussed later, the underground and surface phase change must be avoided due to safety and economical reasons. Both in transportation and sequestration steps, CO_2 needs to be in supercritical conditions. It is costlier to transport and sequester in subcritical conditions. Moreover, it is dangerous and volume consuming in sequestration. Most importantly during sequestration the phase change might end up with rock fracture and damage to the environment [3.16]. The physical requirements for transportation and sequestration are set up by authorities. Sequestration must be carried out at a depth more than 2500 ft to guaranty supercritical condition [3.18]. At this depth 18000 cubic feet of CO2 becomes 50 cubic feet which is 360 times smaller [3.18]. For transportation, according to ASME-ANSI 900# the lower limit is 8619 kPa at 4 C degree and the upper limit is 15300 kPa at 38 C degree. [3.16]

3.3.4 Selection of Site

For the capture-saline aquifer sequestration, we chose Pennsylvania generally. Pennsylvanian saline aquifers have a 75.6 Gigatonnes of CO_2 sequestration capacity.

In western Pennsylvania, below Marcellus shale, there is Oriskany Saline Aquifer at the Appalachian Basins which has most of the Pennsylvanian storage capacity. This aquifer is 300 mile width 600 mile length [3.19]. At Figure 20, there is the depth map of the basin. At the Bureau of Economic Geology, the University of Texas at Austin, several data about the formation such as permeability, porosity, and thickness is available.

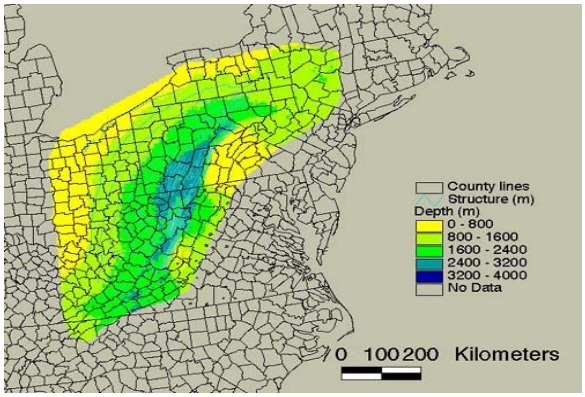

Figure 20: Depth Map of the Oriskany Saline Aquifer [3.14]

Selection of the site depends on several constraints. It should be close to the source, deeper than 2500ft, have a high permeability and porosity. The formation should be thick and the top seal should be highly impermeable although inside the aquifer, it should be continuous. According to the criteria, Indiana County is chosen as the sequestration site. Reservoir properties are shown in Table 8.

Table 8: Formation Properties

Properties	Values
Porosity [3.19]	0.1
Irreducible Water Saturation (assumed)	0.2
Depth [3.19]	3000m (10000ft)
Temperature [3.19]	50 ˚ C (mostly assumed in normal conditions)
Pressure [3.19]	3000psia (20000kpa)
Thickness [3.19]	40 ft
Permeability [3.19]	4-30mD (assumed as 14 mD)
Salinity [3.19]	150 g/l
Top Seal Thickness [3.19]	250-2500 ft

3.3.5 Transportation

Supercritical conditions will be preferred in order to avoid multiphase transportation and because low density fluid transportation is more power consuming [3.27]. Transportation pressure, temperature, cost and pipeline characteristics such as diameter and velocity should be determined.

In transportation, we need to calculate the transportation cost because transportation distance is smaller for saline aquifers compared to other alternatives and this economical analysis might show the advantage of saline aquifers.

The cost is found by using the diameter, pressure drop and the transportation distance. It is assumed that the transportation distance is 100 km (6.2 miles). The diameter needs to be found using some equations which are based on the moody chart. The calculations are explained in the Appendix B.

In our case the CO_2 capture will be $2.79*10^9$ lbs of CO_2 per year 70.76% of which ($1.98*10^9$ lbs/year) will be sequestrated in Saline Aquifers. The mass flux is 32 kg/s (70.4lbs/s) and the diameter of the pipeline is found to be 3.25 ft which will be used for transportation cost in the economical analysis.

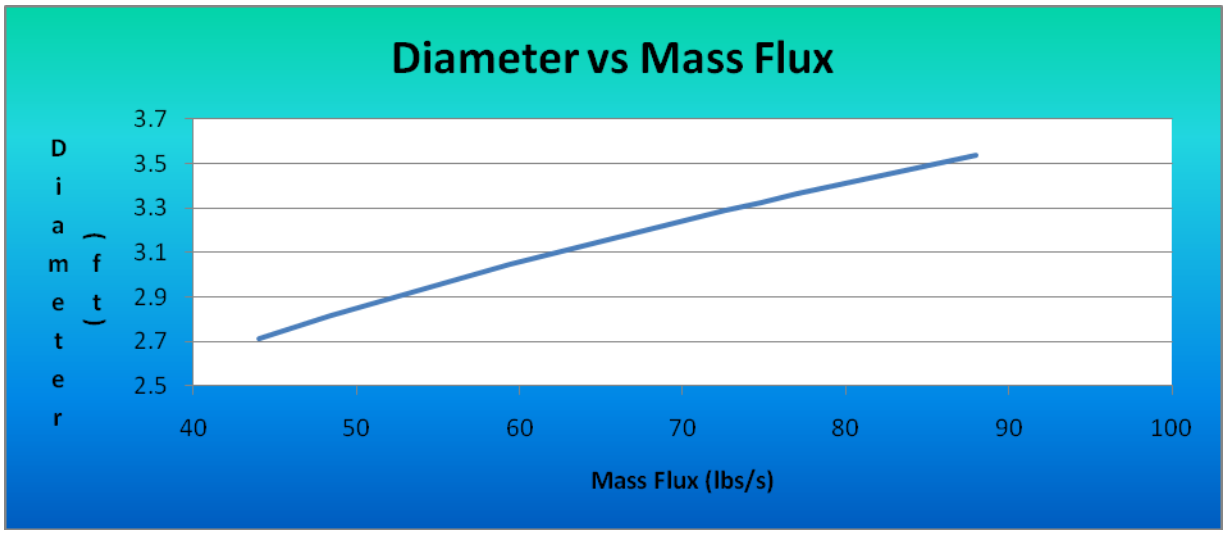

Figure 21: Diameter vs Flowrate

Diameter doesn't increase as much as mass flux does. This is partly because the cross sectional area is increasing directly proportional to the square of the diameter. Mathematically, you can see in the Appendix B that frictional factor and mass flux as well as some other coefficients are not linearly proportional with the diameter.

This diameter analysis will show in the economical analysis that the price doesn't increase as much as the mass flux. Therefore, the unit price of transportation is cheaper when it is transported in large masses.

3.3.6 Formation Fracture Pressure

After transporting the CO_2, another compression is carried out by capturing and later on it is injected into the formation. The condensed gas increases the pressure of the formation within time. Rock can bear pressure until a point. After that, fracture occurs which needs to be avoided. Therefore, the formation fracture pressure needs to be found and the pressure shouldn't exceed fracture pressure.

There are several calculations taking such variables as depth, density into account. The calculations are shown in Appendix B. The fracture pressure is found as 6718 psia while the reservoir pressure is 3000psia at 10000 ft depth.

3.3.7 Pressure Profile

Pressure profile is important in calculating the number of wells, solubility trapping capacity and in seeing the movement of the injection.

As we discussed before, pressure is highest at the injection well. The pressure of the well needs to be simulated in order to detect the time where there is fracturing. If this time is earlier than the life of the project, then another well should be considered to ease the pressure at the well.

The life of the project is 10 years. However, considering that the well can be used for different injection projects or that the project might be extended, the pressure is simulated for 1,000,000 hrs (114 years). Calculations are shown in the Appendix B.

Finally, we can conclude that 1 injection well is not enough. In order to avoid fracture we will use 2 wells. They will be 2000 ft apart from each other.

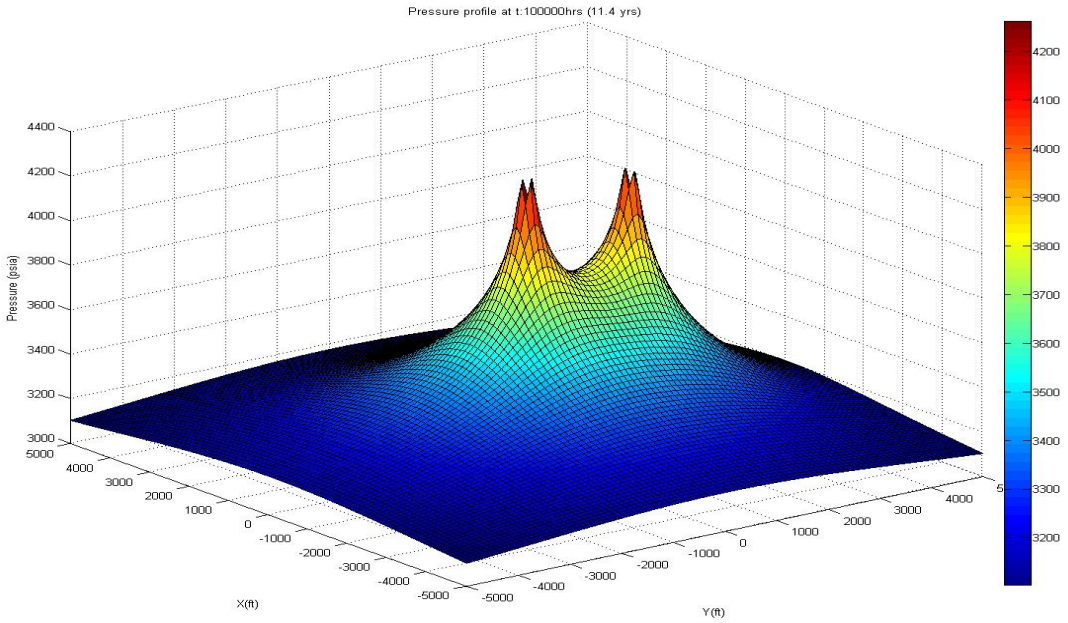

Figure 22: Pressure Profile at t:100000hrs (11.4 yrs)

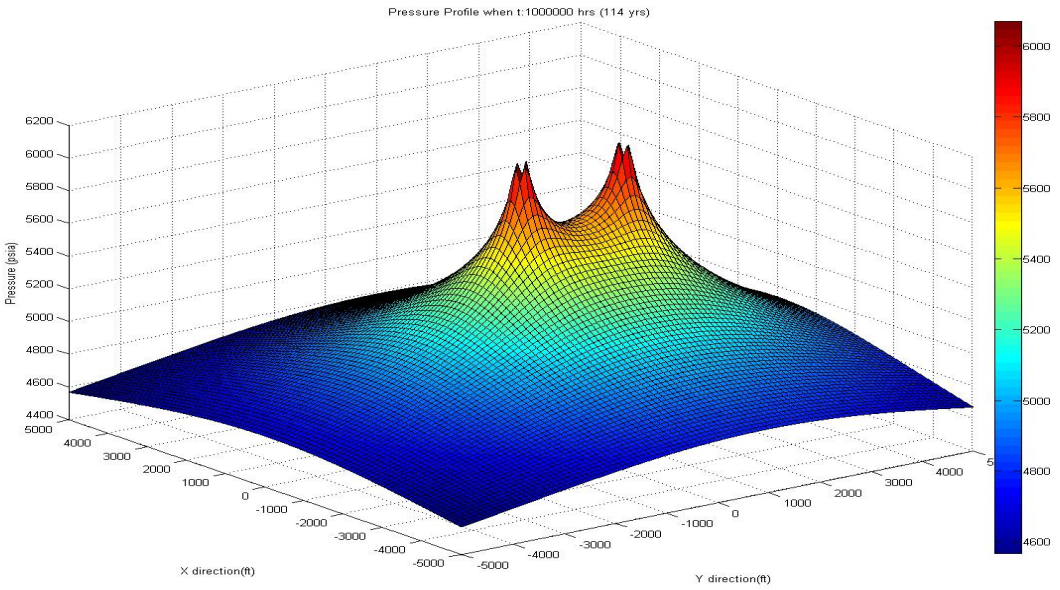

Figure 23: Pressure Profile at t:1000000 hrs (114 yrs)

At t=11.4 yrs, the wellbore pressure is around 4000psia while at t=114 yrs it is around 6000psia which is lower than the fracture pressure.

The pressure profile will help us find a more accurate solubility trapping value because solubility is a function of pressure.

If the same code is run taking a bigger radius into account at 80000ft of radius, the pressure drops below 3500psia. However, the code assumes that the aquifer is infinite. There might be some irregularities which will decrease the permeability and the porosity at some point. It would avoid more dispersion. As I don't have that data, I can't take it into account. Still, we can see that at x=5000ft & y=5000ft, the pressure is around 4000 which is very close to the initial formation pressure. We can assume that, starting from that point, CO_2 won't have a significant effect.

3.3.8 Sequestration Methods

There are several trapping methods which can be divided mainly into 3 as hydrodynamic trapping, solubility trapping and mineral trapping [3.16]. These trapping methods occur naturally.

Hydrodynamic Trapping: Trapping in structural traps. It serves to temporary storage. However, it is needed to start other trapping methods [3.16]. The calculations are shown in the Appendix B. The sequestration capacity is found as 37.2 kg/m^3 (2.32 lbs/ft^3).

Solubility Trapping: Diffusion of CO2 in the aqueous system. Solubility depends on salinity and pressure. The calculations are shown in Appendix B.

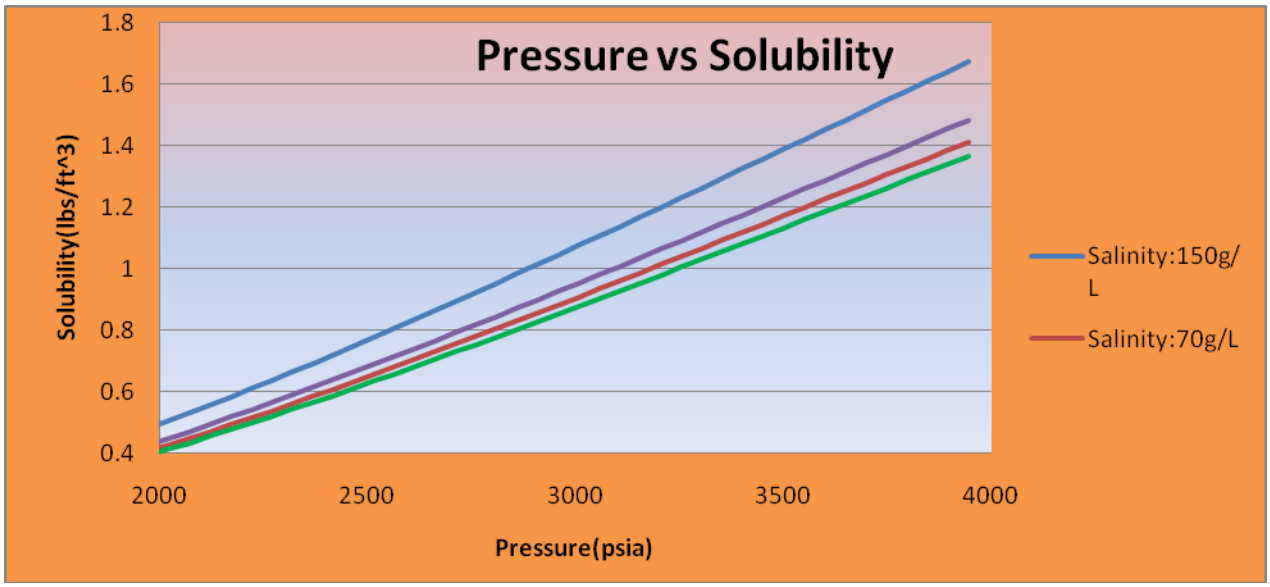

Figure 24: Pressure vs Solubility Graph

In Figure 24 it can be seen that at high salinity and high pressure the solubility increases. Taking the free volume into account, we can find the sequestration capacity as shown in Figure 25.

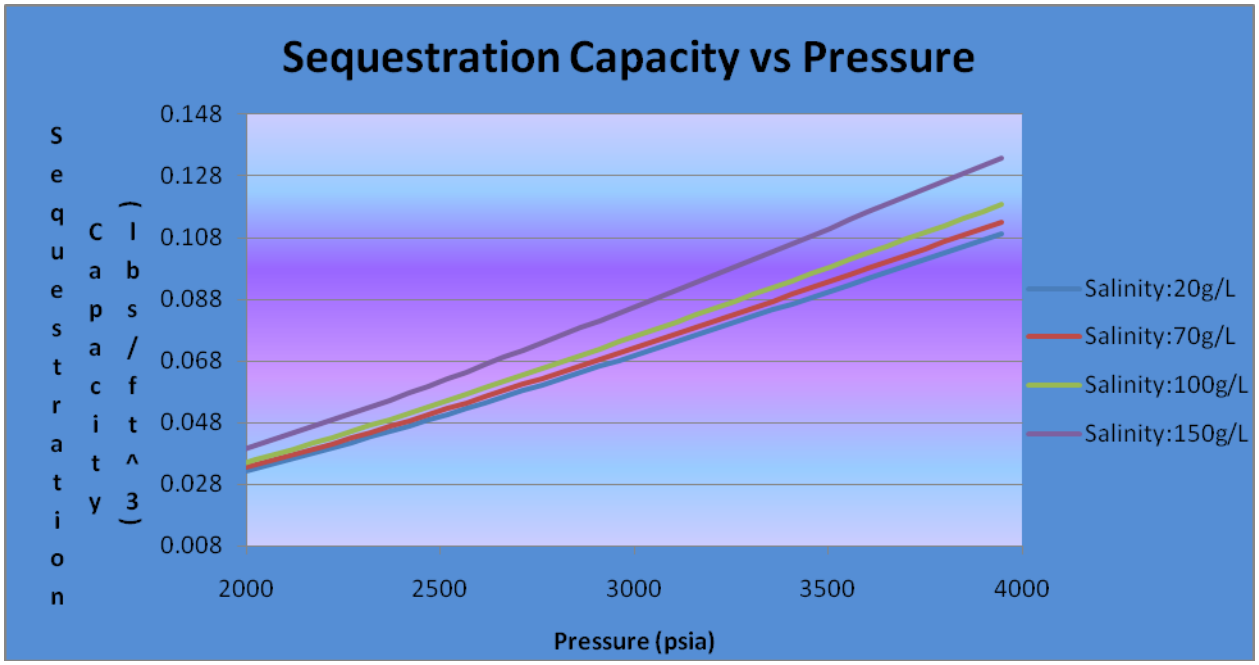

Figure 25: Solubility Trapping Capacity vs. Pressure

Soluble Trapping Profile: Although we assume that the formation pressure is 3000 psia everywhere, after the injection the pressure changes. The pressure profile is already drawn. Knowing the pressure and the relationship between the solubility and the pressure and the pore volume that we can trap CO_2, we can draw the soluble trapping profile. The same calculations in pressure profile and solubility trapping are used.

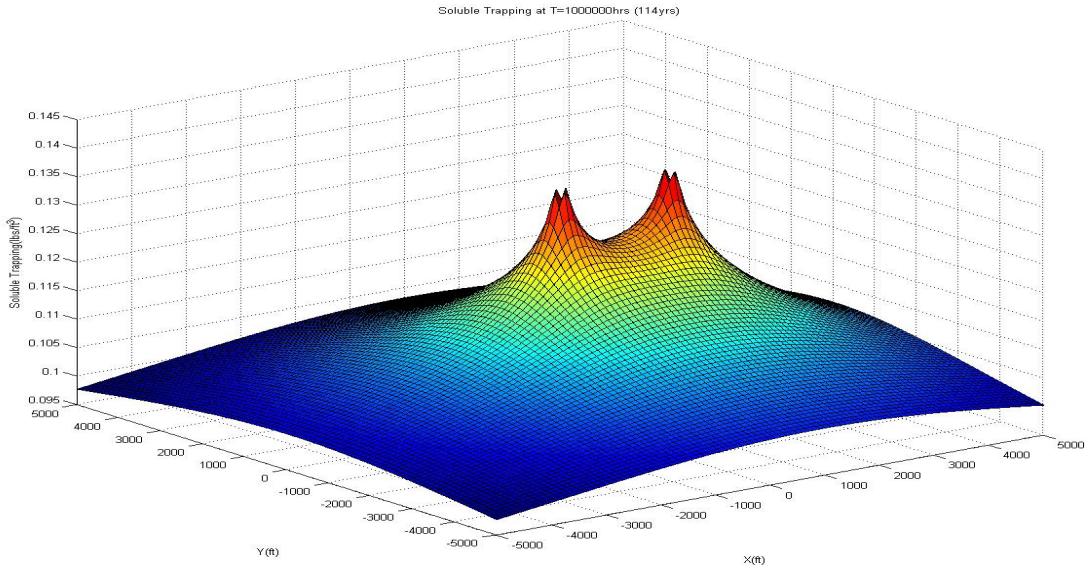

Figure 26: Solubility Trapping Capacity Profile at t=114 yrs

The soluble trapping is between 0.1 to 0.14 lbs/ft^3 for 114 years. However, trapping in free phase is 2.32 lbs/ft^3. It constitutes 4-6% of free phase trapping which is not very significant. On the other hand, my results might not be realistic because I have assumed a lot of things which might have reduced the solubility trapping capacity.

Mineral Trapping: This method traps CO_2 in minerals via chemical reactions. This method is the most permanent method [3.16]. According to Kumar et al. CO_2 leakage can be considerably mitigated if at least most of the CO_2 could be immobilized in gas, dense brine or mineral form [3.24]. However, it might take 1000s of years for it to totally mineralize with natural processes. Still, we can increase the mineralization rate by adjusting its PH before injection. Another negative point is that although it is the most permanent trapping method hydrodynamic and solubility trappings are more pronounced compared to mineral trapping [3.26].

Quantifying the precipitation rate is very difficult because it is very site specific. It depends on the chemical composition of formation waters and of the rock matrix, on the contact surface between mineral grains and the formation water containing dissolved CO_2 and on the flow rate of fluids which are the factors which depend on other several factors such as permeability, viscosity and hydraulic gradients [3.15].

In order to do mineral trapping, firstly hydrodynamic trapping needs to occur. After the hydrodynamic trapping, CO_2 reacts with other minerals to form another mineral. With mineral trapping, calcite, dolomite, siderite and magnesite can be formed. According to the sample taken from the site, PH has more influence on mineralization rather than pressure and temperature. Below there are the series of chemical reactions that will take place underground [3.21].

1) $CO_2(gas) <--> CO_2(aq)$

2) $CO_2(aq) + H_2O <--> H_2CO_3$

3) $H_2CO_3 <--> H^+ + HCO^-_3$

4) $HCO^-_3 <--> H^+ + CO^{2-}_3$

5a) $Ca^{++} + CO^{2-}_3 <--> CaCO_3\ (Calcite)$

5b) $Ca^{++} + Mg^{++} + CO^{2-}_3 <--> CaMg(CO_3)_2\ (Dolomite)$

5c) $Fe^{++} + CO^{2-}_3 <--> Fe(CO_3)_2\ (Siderite)$

5d) $Mg^{++} + CO^{2-}_3 <--> MgCO_3\ (Magnesite)$

At high PH such as 11, there will be a lot of OH^- in the environment which will increase the mineralization. When the OH^- is consumed, the mineralization slows down.

Dilmore et al. uses bauxite residue to increase the PH of the formation. In their studies they find that 9.5g/l of CO_2 can be sequestrated in this method.

The aquifer's geological data is as follows: Ca (mg/L): 25133, Fe (mg/L): 165, Mg (mg/L): 1540 and the PH is 2.72 [3.23]. Using this data and the below equation, we can find the precipitation rate. [3.16] The fact that PH is low is very bad because it will slow down the mineralization.

Mineral trapping is insignificant in hundred years with natural processes. Normally, it takes thousands of years due to the low precipitation rate. However, they can be stimulated by increasing the *pH* of the ambience. With natural trapping, precipitation will decrease the *pH* and acidify the aquifer which is dangerous. This is another reason for the necessity of the *pH* adjustment. *pH* can be increased using concrete which is a construction waste and which has mostly $Ca(OH)_2$ [3.28].

In this project, *pH* of CO_2 in the formation is assumed to be constant. Natural mineralization will also occur in the formation. You can find the calculations in Appendix B.

Results: The trapping capacity 50 years after the first injection is as below. 100 years later capacity will double. In real case, the precipitation would be getting lower because of the decrease in PH, permeability and porosity due to the mineralization taking place:

Table 9: Mineral Trapping Capacity

Mineral	Mineral Trapping (kg/m3)	Mineral Trapping (lbs/ cubic ft)	% of total trapping
Calcite	0.013244066	0.000826801	0.035637955
Dolomite	0.544913495	0.03401786	1.466287055
Siderite	0.013811216	0.000862207	0.037164077
Magnesite	0.003667171	0.000228934	0.009867851
Total	0.575635948	0.035935801	1.548956938

Interpretation for Trapping Methods:

Most of the mineral trapping will be in dolomite due to its high rate constant. However, at the end of 50 years only 1.54% of CO_2 will be able to be mineralized. 4-6% of total CO_2 will be able to be sequestrated via solubility trapping. The rest which is around 92.5-94.5% will be in free phase. The free phase is not necessarily mobile not to mention the thick impermeable seal. However, dip angle and other characteristics need to be examined to check its mobility.

The values for my solubility trapping and mineral trapping might or might not be realistic because a lot of assumptions have been made. Still, by looking at the literature review some concerns can be derived.

Concerns and Assumptions:

1. Permeability and porosity reduction will affect other types of trapping methods.
2. PH change might affect environment. Increasing the PH both increases the mineralization and eases the danger to its environment.
3. With natural methods, there is no significant trapping in 50 years.
4. The ion activity product changes with time is ignored.

3.3.9 Leakage

Although the aquifer is sealed by highly impermeable Devonian shales which has a 1500 ft thickness [3.25] and the permeability of which is expressed in terms of nanodarcy, there will still be some leakage which can be neglected. Still, the leakage should be quantified. The calculations are shown in the Appendix B. Finally $Q_{leakage}$ is $2.62*10^{-6}$kg/s (0.000113% of total CO_2) which is insignificant.

The aquifer is below the Marcellus shale. Therefore, I assume the abandoned wells are not as deep as the saline aquifer. Therefore, I assume that there is no leakage from abandoned wellbores. However, in real case, they should be found and fixed properly for CO_2 sequestration.

3.3.10 Environmental Risks

There might be leakage from the seal or the abandoned wells. Leakages might damage crops, groundwater quality, human and animal health. High CO2 concentration changes the biogeochemical properties of the soil; it changes PH, replaces O2, affects subsurface fauna. In case of leakage to the atmosphere, it might lose its climate change mitigation effect and damage people, crops and animals if there is not much wind at the place. In case of mixing with groundwater flows, it will increase the CO2 concentration of the water.[3.17] To avoid damage, vulnerable areas should be avoided, injection process should be monitored, remote sensing techniques should be used and water quality analysis should be carried out.[3.17]

3.3.11 Monitoring & Mitigation

Modeling should be carried out before injection in order to estimate the geological, chemical and physical situation in different times. We can name these models as CO_2 behavior models which are reservoir models, geochemical models, geomechanical models, CO_2 equation of state at reservoir conditions. After injection, plume tracking should be applied. It is done mostly by the seismic techniques. They are surface to borehole seismic monitoring, micro-seismic monitoring, cross well tomography, reservoir pressure monitoring, observation well/fluid sampling.[3.22]. The aim of the monitoring is not only to investigate the leakage but also to check whether the project has been successful. These tracking systems emit sound waves and later on these waves are reflected by the reservoir. These returning sound wave properties such as velocity give us information about the geological position of the CO_2. This way, we can know whether CO_2 leaked [3.16]. Another way of monitoring is taking samples from the reservoir and its ambience. Monitoring vegetation growth rate, examining water, air and soil CO_2 concentration, using subsurface monitoring wells may give information about the CO_2 leakage. In case of leakage, the project will be failed and the target zone will be depressurized [3.22].

3.3.12 Economical Analysis

"*The capital cost of sequestration can be divided into cost of transportation and cost of storage*" [3.29] CO_2 compression cost is included in the capture section.

Transportation Cost:

Transportation cost is a function of pipeline length and diameter. I assumed 100km of transportation. Calculations can be found in Appendix B. Finally, we can have 4 different types

of cost values such as ROW (Right of Way), Labor, Miscellaneous and Material costs. Right of way cost is "*the cost of obtaining right-of-way for the pipeline and allowance for damages to landowners' property during construction*"[3.29]. The cost values for different flow values can be graphed.

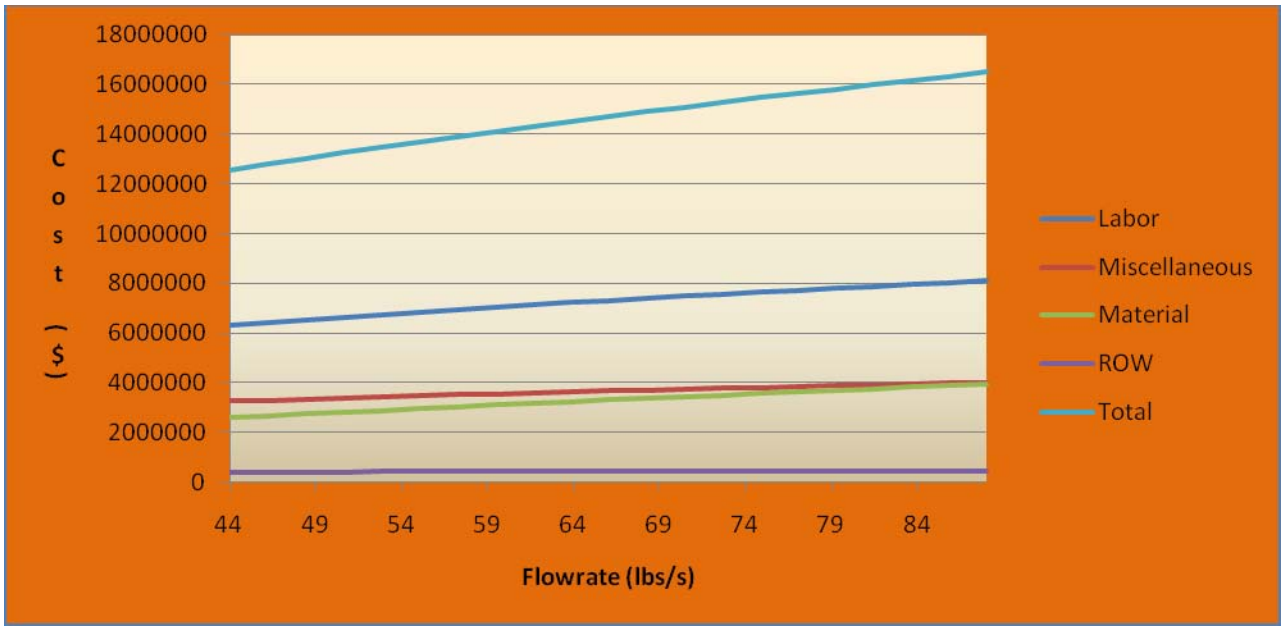

Figure 27: Transportation Cost vs Flowrate

The flowrate is 70.4 lbs/s. The corresponding capital cost becomes $15,092,709.

Drilling Cost:

According to Snead [3.30], the cost of injection drilling is $83.98/ft for depth between 5000-10000 ft and $142.56/ft for depth between 10000-15000. With interpolation, we find $113.27/ft for 10000 ft depth. The cost for 1 well at our depth becomes $1,132,700. It makes $2,265,400 for 2 wells.

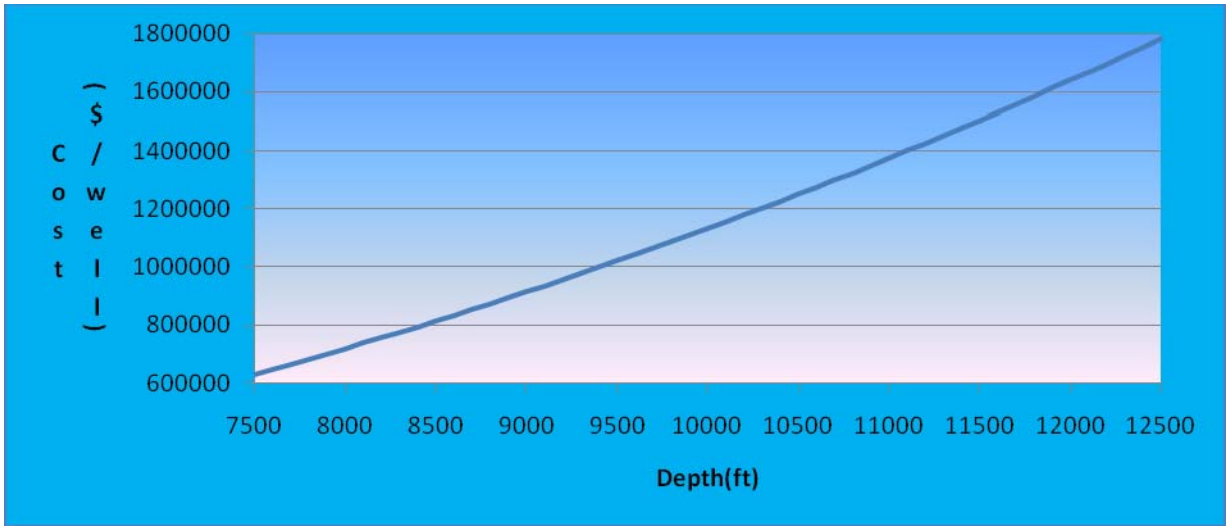

Figure 28: Well cost vs Depth

Cost Analysis: Compression before injection cost will be included in sequestration part. The pressure needs to be increased from 1500psia to 3000 psia. According to the capturing part the cost is 0.0016$/ton CO2 for each psia increase. The annual operating cost is 10% of the capital cost. Payback period is 10 years and the interest rate is 5%.

Table 10: Cost Analysis

Transportation **cost($)**	**15,092,709**
Well #1 ($)	1,132,700
Well #2 ($)	1,132,700
Total Capital Cost ($)	17,358,109
Net Present Value ($)	1416988.49
Operating Cost ($)	141698.849
Yearly Cost ($)	1558687.339
Unit Cost ($/ton)	1.544552
Unit Cost with Compression ($/ton)	3.944552
Unit Cost with Compression ($/lbs)	$1.97*10^{-3}$

Finally, unit cost becomes $1.54/ton of CO_2 without considering the compression. In another paper that is compared, the sequestration cost is between $7.5-15/ton [3.29]. This is mostly because my transportation distance is little and I need fewer wells for more CO_2 sequestration. In my pressure profile, I assumed that the formation is infinite which kept the pressure low. This might have caused a comparatively fewer well number requirement. Moreover, my porosity and permeability values might be a lot higher than an average saline aquifer. Moreover, cost of drilling in my reference is a lot higher because of high off shore drilling costs.

3.3.13 Sensitivity Analysis

Using the same equations, we can calculate the unit price of CO_2 for different parameter. For example, if the transportation distance is increased to 100km, then the unit cost of CO_2 sequestration becomes \$13/ton of CO_2.

We can calculate the unit cost for different flowrates as well. Only 1 well will be needed for 25% lower flowrate. Therefore if the flowrate is less than 52.8 lbs/s, 1 well will be enough. Moreover, transportation cost will change with flowrate. Finally, we can conclude that the sequestration cost decreases with the increase in flow rate.

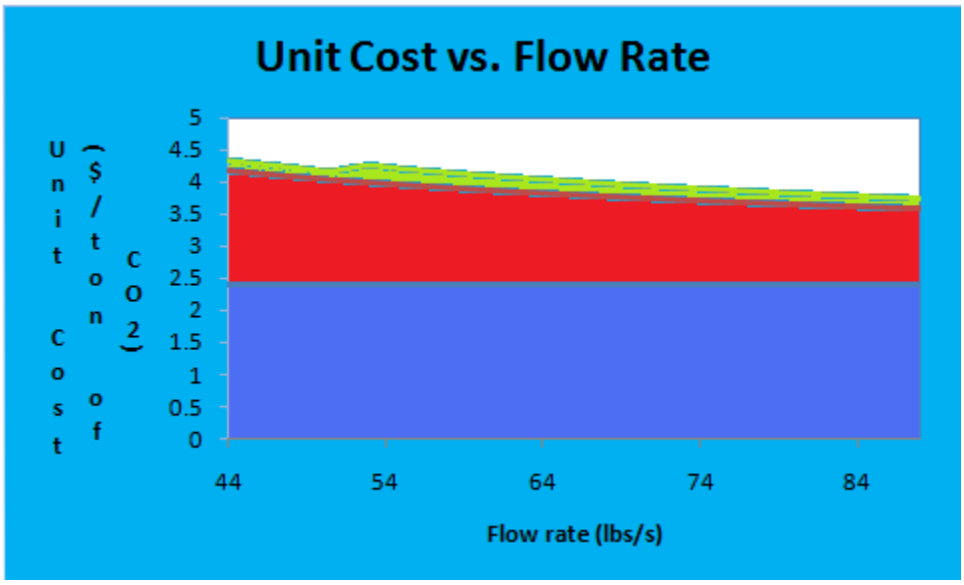

Figure 29: Unit Cost vs Flowrate (Blue represents the compression cost, red represents the transportation cost, green represents the well cost)

Chapter 4

Utilization of CO_2

4.1 Introduction

Carbon dioxide (CO_2) can be found in the atmosphere as a result of natural occurrence or as a waste of industrial process. In order to limit the effect of CO_2 emission in the environment, it must be utilized as a resource for useful application in the industrial or commercial process.
It has been proved through experimental work, that CO2 can be applied in the industrial business as an EOR fluid that is capable of enhancing the oil recovery. In addition, it can be a great substance in the commercial process in fields such as, fabric cleaning, fire extinguishers, and in the making of wine.

In this project, CO_2 will be utilized in the industry as an injection fluid to enhance oil recovery in oil reservoirs after the pressure is no longer supporting the recovery of the hydrocarbons. Typically oil fields produce 20-40% of its oil reserves using conventional methods under the support of reservoir pressure and the implementation of enhanced oil recovery techniques such as CO2 cycling, could provide 30-60% of recovery increase [4.1].

4.2 Carbon Dioxide for Enhanced Oil Recovery (EOR)

Oil reservoirs are subsurface pools of hydrocarbon contained in porous media and surrounded by low permeability rocks [4.2]. Reservoirs typically contain Original Oil in Place (OOIP) which is defined at the exploration stage of the extraction process. The OOIP helps in defining the amount of oil that has been produced and the amount of oil that is left in the reservoir, it also works as an assessment measure for future recovery plans.

Naturally, the production of the oil in place is controlled by nature since the lithology of the reservoir and the properties of oil at different pressure and temperatures are the factors of extracting the oil from the reservoir; oil could be at a low viscosity that prevents it from flowing, or it could be strongly attached to the grains inside the pore spaces where it is unreachable. Thus, in order to make the oil more soluble and easy to be transported to the perforation zones where the production starts, a mechanism has to take place to lower the viscosity of the oil and apply a force to push it to the production zones. In this case, the best method to be implemented is by using CO_2 as an injection fluid to enhance the recovery of the oil.

Since there are not any CO_2-EOR Techniques applied in the region of Pennsylvania and considering the importance of this approach to reduced the CO_2 emission, a recovery approach will be implemented using CO_2 gas injection to enhance the recovery of a reservoir that has OOIP of about 200 MSTB, with 40% of OOIP produced and 120 MSTB of the reserves are unrecoverable using conventional recovery methods.

4.2.1 Fundamentals

Carbon dioxide exists in different types of fluid phases based on pressure and temperature. It can be found as gas, liquid, solid or supercritical fluid. Generally, it is preferable to use CO_2 in the supercritical state in operations such as enhance oil recovery because it is more stable above the critical conditions [4.1].

Carbon dioxide is a major greenhouse gas and the purpose of this study is to utilize it in order to eliminate the damage caused by its emission. Transforming CO_2 into a supercritical phase is very useful in the EOR technology for economical and environmental purposes. The EOR will eventually increase the oil production or at least accelerate the production of oil with time. Recycling CO_2 after the EOR, for future usage, will prevents the impact of CO_2 on the environment.

The supercritical condition can be defined as the state where the pressure and temperature have exceeded their critical conditions at which the properties of the gas and liquid phases are identical [4.3]. Figure (3.2.1) represents the pressure-temperature diagram of the phase behavior of CO_2. The critical conditions for CO_2 at which there is no distinguish between gas and liquid exists at a pressure of 7.38 Mpa and at a temperature of 31.1 ^{o}C.

At Supercritical conditions, the fluid experiences low surface tension than liquids which allows it to diffuse more easily along surfaces with regular and irregular geometry, and through small pore spaces [4.4]. In addition, the supercritical fluid still performs as a liquid in terms of density and as gas in terms of viscosity [4.1].

4.2.2 Applications

Carbon Dioxide is used for the purposes of EOR in a traditional practice which involves miscibility with the oil, or as immiscible which involves risky operations and is not yet a common practice due to limitations [4.5]. In this project, CO2 will be utilized with traditional technology available.

Miscible CO_2 displacement is commonly and favorably applied in light oil reservoirs found at depths greater than 3000 ft and with high gravity exceeding 25 ^{o}API [4.5]. Thus, during injection under suitable depth and density, CO_2 will mix thoroughly with the oil causing the loss of all interfacial tensions which will allow miscibility between the two substances. Theoretically, all the oil should be extracted as a result of the miscibility conditions, but actual practices has showed that only 10 to 15% of OOIP can be added to the overall recovery [4.1].

At this point, CO_2 is mixed with the oil in which both are miscible with each other, meaning that oil is no longer attached to the grains of the reservoir and is waiting for a mechanism to push it to the production zones. Commonly, water drive is used as a driving force in a process called water-alternating-gas (WAG). The process is achieved by repeatedly alternating the injection of CO_2 with water injection to enhance the oil recovery as illustrated in Figure 30.

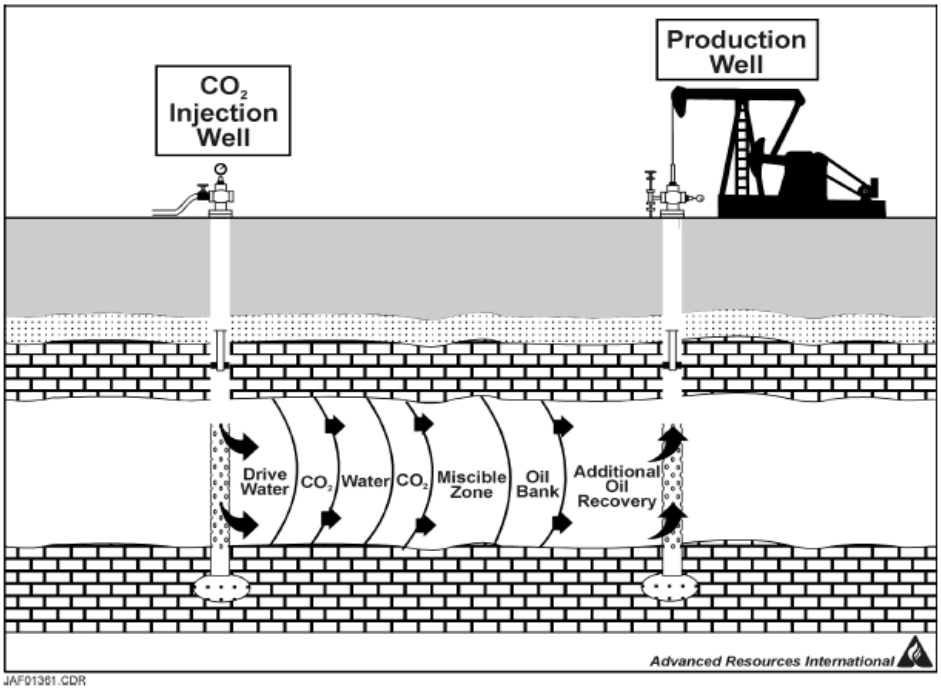

Figure 30:CO2-water flooding [4.1]

4.2.3 System Design and Process

Figure 31 represents a typical surface configuration of an enhance oil recovery process [4.1]. The process of the CO_2-EOR starts with establishing connection channels with a source of CO_2 from a fossil plant, which is expected to feed the recovery project until ultimate results are achieved. The transportation of the CO_2 will be established through pipelines, which will be connected to the injection wells at the site.

Once injection is conducted and the break though has taken place; oil, water, and CO_2 will start to be produced through the production wells. All the fluids coming out of the production wells are connected through pipelines to separation vessels, which are responsible for separating the oil, water, and CO_2.

The first stage of separation will separate the gas from the liquid, resulting in extracting CO_2 and sending it back to the recycling compressors for re-injection purposes. The fluid which contains the water and oil will be sent to a second separator vessel to separate the oil and the water.

As the separation takes place, the oil will be sent to storage facilities for further treatment or sales, and the water will either be sent back for Water-Alternating-Gas purposes or will be disposed through disposal wells. At this point, all the ends are connected and the cycle of the CO_2 EOR operations is concluded.

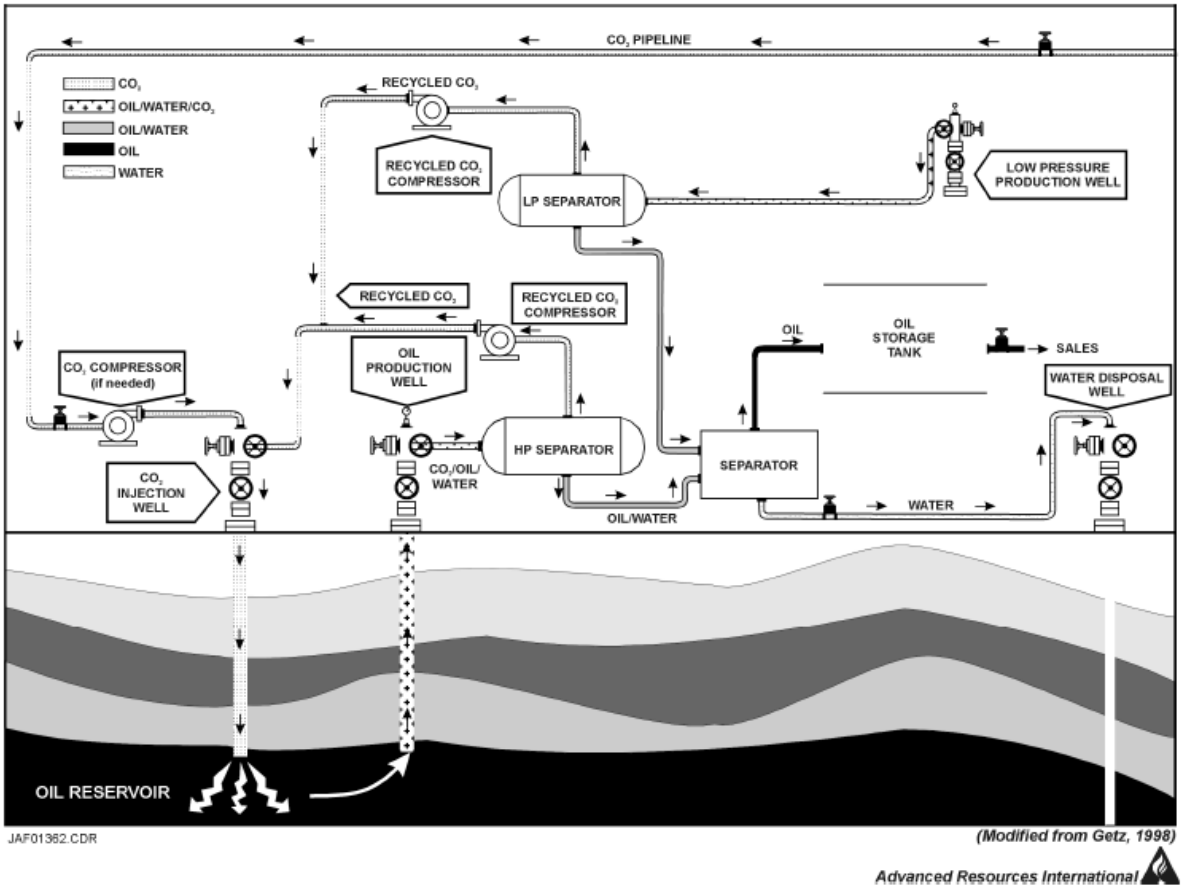

Figure 31: Typical CO2 EOR field operation

4.2.4 Technical Limitations

Efficient recovery of oil using CO_2 injection is basically dependent on understanding the fluid properties of oil and CO_2 and the behavior of both fluids as they come in contact.

As the CO_2 is injected in an oil reservoir, it mixes with the oil, where the behavior of the mixture is dependent on the concentration of CO_2 and the pressure. Figure 32 illustrates the behavior of a binary mixture below 120 ^{o}F of CO_2 and oil from the Wasson field, a large field in West Texas where CO_2-EOR is planned [4.6].

As illustrated in the plot, at 0.0 mol % CO_2, the oil is liquid at pressure below 900 psia, and it splits into two phases as the pressure drops below 900 psia. In the other hand, at 40.0 mole % CO_2 concentration, a liquid and vapor phase is formed below 1350 psia and only liquid phase is formed above the same pressure [4.6].

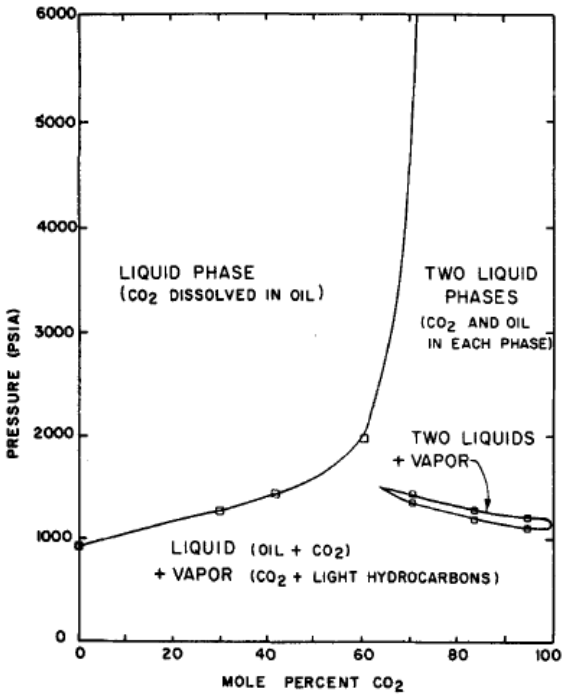

Figure 32: Binary mixture behavior of CO2 and Oil at 120F

According to the plot, it is clear that the CO_2 is soluble in oil at a typical reservoir pressure but as the CO_2 concentration increases with pressure, the phase behavior is more complex. For example, at 2500 psia, the concentration of CO_2 must not exceeds 0.7 mol %, otherwise high pressure is needed to force all the CO_2 to be dissolved in the oil [4.6]. As a result, the oil expands as more CO_2 dissolves in it. In addition, as the CO_2 is injected and comes in contact with oil, it dissolves in the droplets of oil and occupies some volume allowing the oil to swell. Figure 33 shows the increase of swelling factor of oil as the concentration of CO_2 increases in the mixture [4.6].

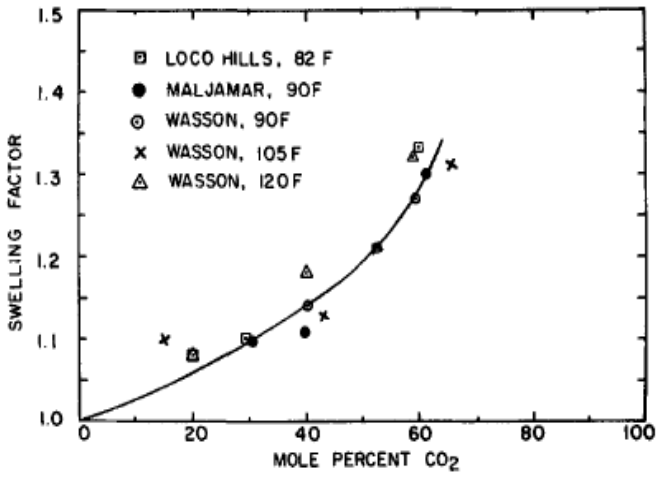

Figure 33:Swelling factor of oil

Thus, as the oil droplets swell, they will merge together to unite in one body of fluid which will allow it to flow more easier to reach the production zones. However, the amount of oil which can be mobilized by swelling is limited to the oil which has greater saturation than the residual oil indicating a mobility problem [4.6].

In addition, another displacement issue revolves around the variety in viscosity measures between the CO_2 and oil as they come in contact. As the CO_2 is dissolved in the oil, the viscosity of the resulting mixture is lower than that of the original oil indicating a viscosity instability displacement and a reduction in the mobility of the oil.

There are two types of displacement in the flooding process, stable and unstable displacement depending on the difference between the viscosity of the sweeping and the residual fluid. Unstable displacement is formed when the viscosity of the sweeping mixture is less than the residual fluid, while the stable displacement occurs when the viscosity of the displacing fluid is equal or higher than the residual fluid [4.6]. Figure 34 illustrates the difference between the stable and unstable displacement.

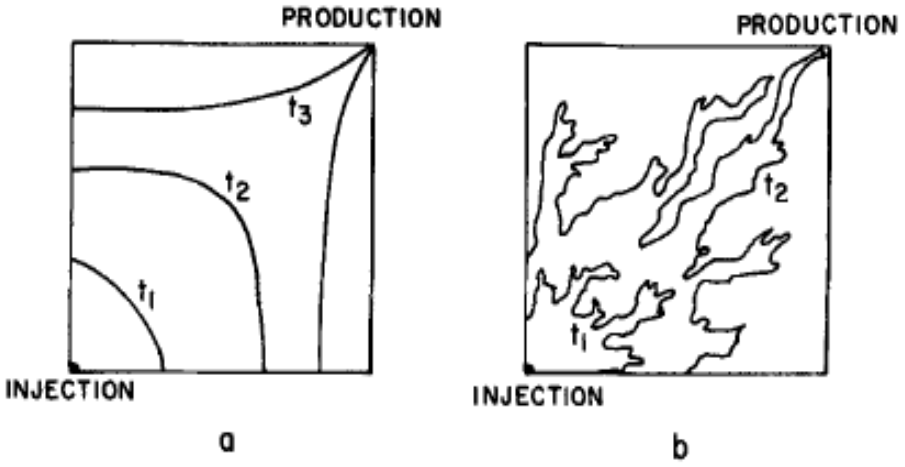

Figure 34: Comparison of stable and unstable displacement [4.6]

Figure 34(a) and 34(b) represent a two dimensional reservoir with two wells in each corner; the injection well is at the bottom left of the reservoir and the producing well is on the upper right-hand corner. As the injection process start, the displacing fluid advances through the porous medium toward the low pressure region, where the producing well is located. If the viscosity of the injection fluid is greater or equal to the residual fluid, a uniform advancement of the sweeping fluid will occur as illustrated in figure a. Thus, at time t3, when the injected fluid breaks through into the producing well, most of the reservoir has been swept.

In the other hand, figure b represents a situation where the viscosity of injected fluid is less than that of the reservoir fluid. In this case, an irregular displacement front with developed fingers will occur, causing early breakthrough of CO_2 to the production well. The viscous fingers at t1 starts small and it keeps growing as more injection take place. At t2, an early break through occurs and at this point only few reservoir fluids have been swept due to the non-uniformity in displacement. As a result, a major reduction in the recovery of the reserves will be experienced due to the unstable conditions of the displacement [4.6].

In order to eliminate the growth of the viscous fingers, a reduction in the injection rate and an increase in the pressure gradient behind the frontal region of the injection fluid most be applied. Unfortunately, this approach will cause the production rate to drop.

One approach to control the mobility and also have great sweep efficiency is to apply Water-Alternating-Gas (WAG), Figure 30. This approach will decrease the relative permeability to the injecting fluid by introducing a small increase in the water saturation. As the water is injected with the miscible fluid, water will fill up the pores that were previously available for the CO_2 which will cause the mobility for the CO_2 to decrease [4.6]. In addition, an increase in the pressure behind the frontal region will increase which will develop a uniform advancement of the

sweeping fluid. In conclusion, WAG will help in controlling the CO_2 mobility and increase the efficiency of sweeping which will result in more and enhanced recovery of oil.

4.2.4 Engineering Approach

In this project, the data of a field found in New Mexico were considered as a candidate to be the properties of a hypothetical reservoir in Pennsylvania (see Appendix A for the engineering analysis). The fluid and rock properties were used in the building of a reservoir simulation model utilizing CMG simulator to address key issues and evaluate the enhancement in recovery using CO_2-EOR. Basically, the model utilizes five (5) wells, one well is an injection well and the rest are considered production wells. Figure 35, represents the field with the wells in place.

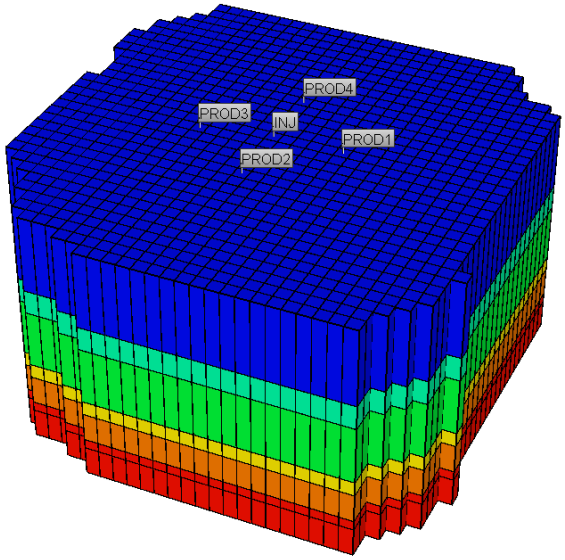

Figure 35: 3-D representation of the field

In this section, the displacement and breakthrough time of CO_2 will be evaluated to measure the impact on the performance of the reservoir. The approach to achieve the anticipated results will be through setting the injection well to be injecting at a rate of 70 million cubic feet per day, while allowing the production in the producing wells to be driven by the pressure. This approach will allow us to address the objectives of the study.

4.2.5 Results

The simulation model was run for 10 years to predict the movement of CO_2 and the ultimate recovery of oil from the hypothetical reservoir. Figure 36 represents the movement of CO_2 as injection takes place.

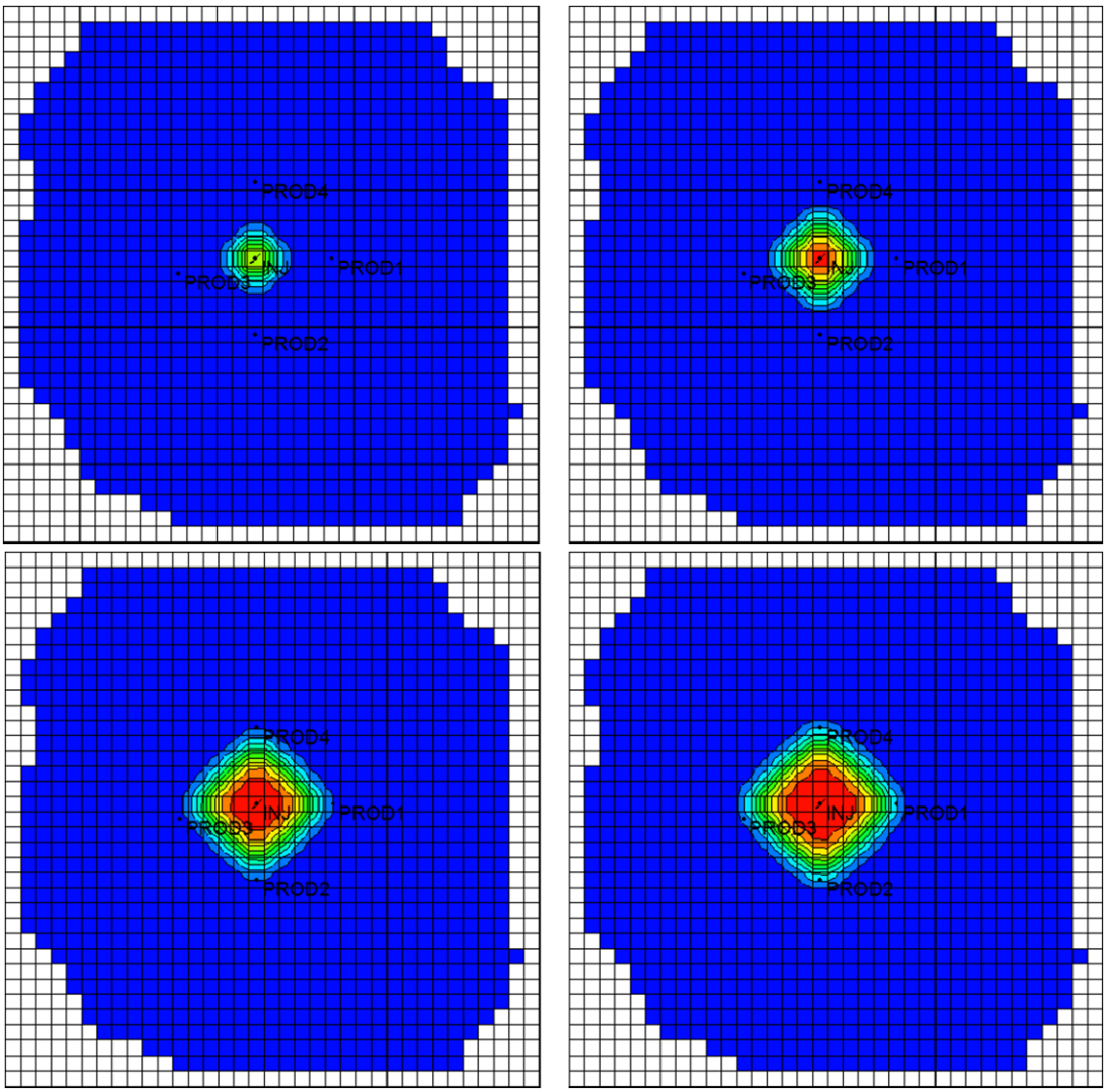

Figure 36: Displacement of CO2 as a sweeping fluid

Comparison between the plots in figure 36 shows the CO_2 injection frontal region as it advances towards the production wells under the specified conditions of the reservoir. The monitoring of the sweeping fluid movement shows that a uniform displacement has been achieved and an ultimate recovery of the residual fluids had taken place.

During injection, the CO_2 tends to fill in the pore spaces and pushing the oil forward toward the production zones, where the production wells will sense an increase in production rate due to the increase in pressure gradient between the sweeping and residual fluids. The increase in production rate will keep increasing until a break through takes place representing

that most of the residual fluids has been swept and the injection fluids will tend to cycle through the reservoir.

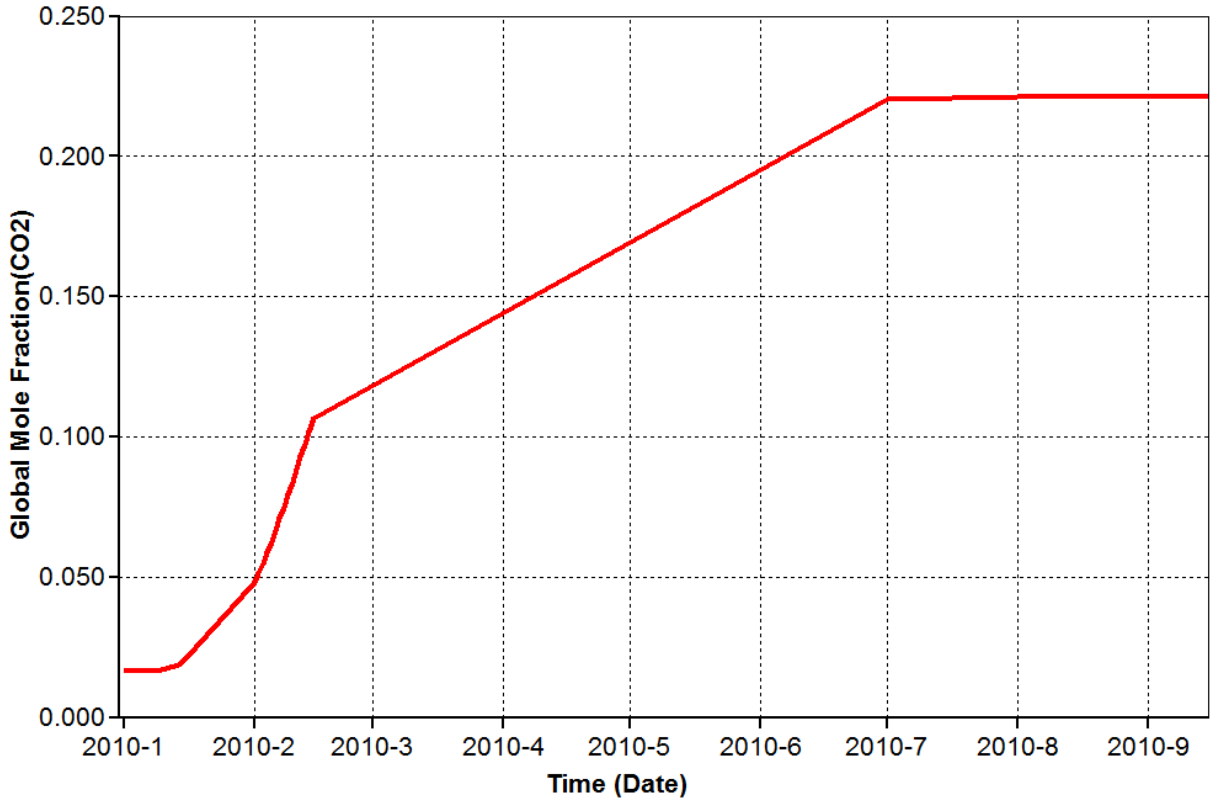

Figure 37: Global mole fraction of CO2

Figure 37 shows the CO_2 mole fraction in the production wells. The CO_2 breaks through in about 5 years from the commencement of injection. The inclined section in the plot which covers a period of four months and 10days, represents the sweeping period of the residual fluids. While the plateau represents that ultimate recovery using CO_2-EOR has been achieved. However, the ultimate recovery from CO_2-EOR should not be interpreted as the final recovery of hydrocarbon and that there are no residual fluids left behind. The method implemented in this study is only expected to add a recovery of 30-60% of the hydrocarbon left behind after primary recovery, while further enhanced recovery techniques can be implemented to add more recovery depending on the reservoir properties.

Figure 38 shows the field cumulative oil production by CO_2 EOR depletion. As the CO_2 breaks through, the cumulative oil production increases significantly, because the injected fluids keep the formation pressure higher than that in the reservoir. The inclined section of the plot represents the sweeping period where most of oil is recovered. The plateau represents ultimate recovery of oil, which is 43.0 MSTB. Considering the initial conditions of the reservoir, where the OOIP is 200MSTB with 40% of OOIP produced and 120 MSTB of the reserves are

unrecoverable using conventional recovery methods, the CO_2-EOR has increased the recovery of the residual oil by 35.8%.

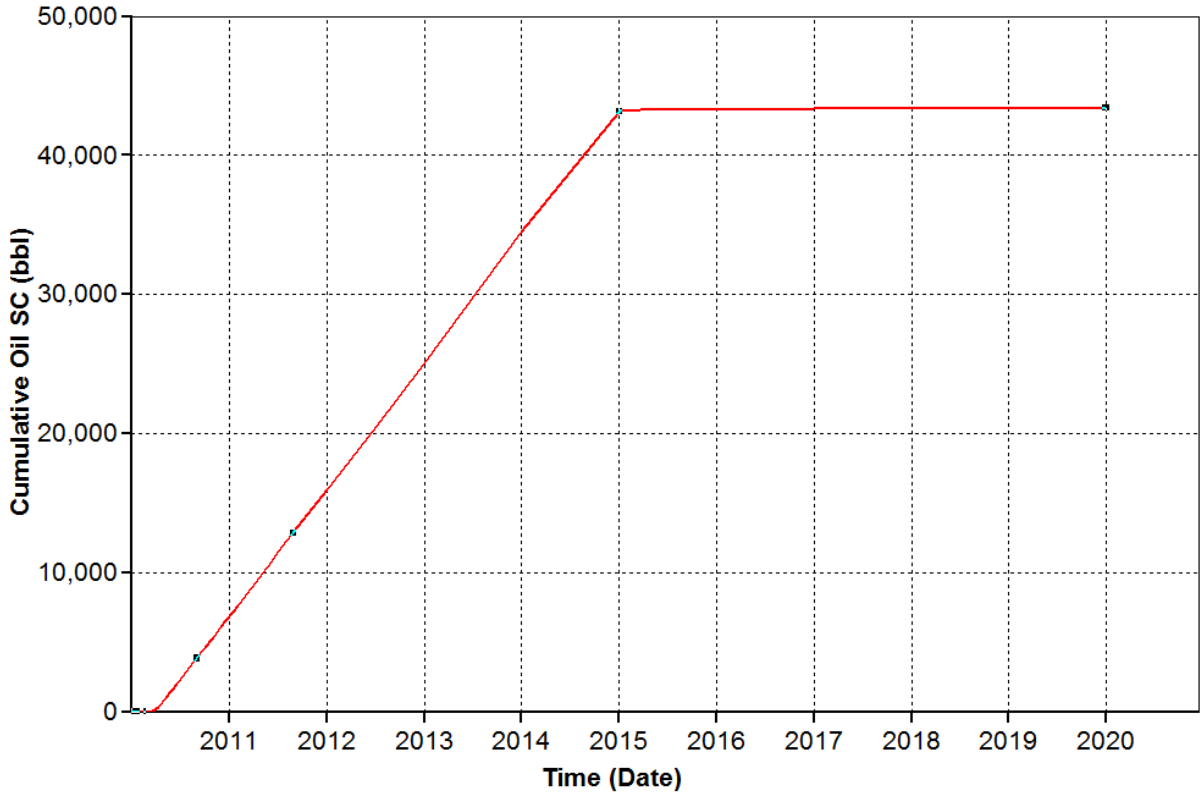

Figure 38: Cumulative oil production

The cumulative gas injected and produced can be seen in Figure 39, which shows that after year 2015 CO_2 break through, the gas rate does not change and it becomes constant. The plot shows that the cumulative CO_2 injected becomes parallel with the cumulative CO_2 produced, indicating that the CO_2 is cycling in the five wells. This represents that once ultimate recovery has been achieved; there are no reason to keep injecting and producing because no further recovery will be produced. Thus, ultimately the operation of CO_2-EOR should be concluded at the end of year 2015, reducing a period of 5 years of injecting and producing.

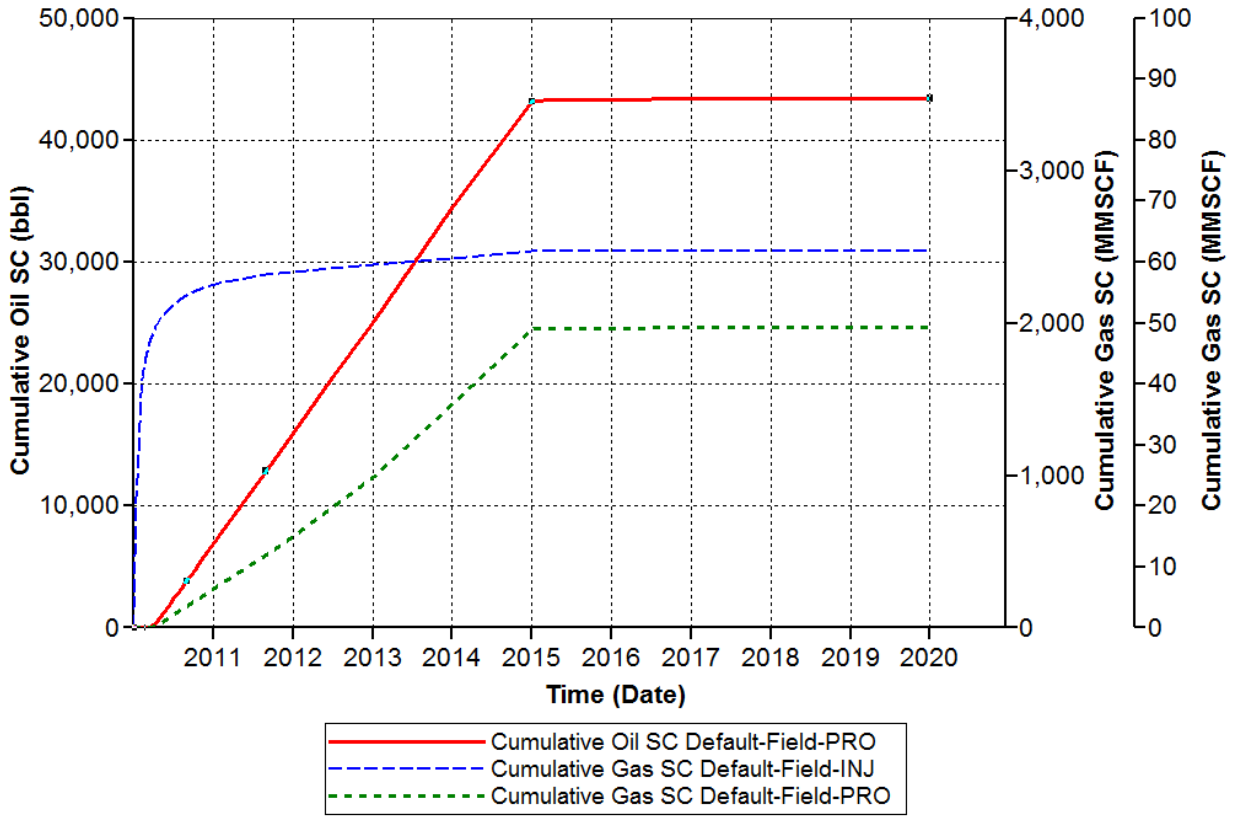

Figure 39: Cumulative gas injection and production

4.2.6 Economical Analysis

The purpose of the economic analysis is to evaluate the feasibility of CO_2-EOR as an optimization method to increase oil recovery through obtaining a net cash flow and comparing it to the expenses of the process. The main revenue in the analysis is coming from the recovery of the 43.0 MSTB of oil that has been produced as a result of the CO_2-EOR process. While the largest expenses will be from the purchasing of CO_2, recycling, and the operating and maintenance cost of the project. In this study, the cost of building recycling plants and construction pipeline network will be ignored based on the assumption that those facilities are already established.

The economic analysis in Table 7 is based on the estimated recovery, residual oil in-place, oil price, and operating costs of the CO_2-EOR process.

Table 11: CO2-EOR cost table

CO2 Injected		(MMcf)	2400
H2O Injected		(Mbw)	0
Oil Produced		(Mbbl)	43
H2O Produced		(MBw)	0.85
CO2 Produced		(MMcf)	50
CO2 Purchased		(MMcf)	0
CO2 Cost	$1.50/Mcf	($M)	0
CO2 Recycled		(MMcf)	50
CO2 Recycle Cost	$0.40/Mcf	($M)	20
Oil Price		($/Bbl)	45
Gross Revenues		($M)	1935
Royalty	12.50%	($M)	241.875
Severance Taxes	1.00%	($M)	19.35
Net Revenue		($M)	1653.775
CO2 Recycling Plant		($M)	0
Wtr Recycling Plant		($M)	0
Trunkline Construction		($M)	0
Operating & Maintenance		($M)	60
Lifting Costs	25%	($/bbl)	23.4625
G&A	20%		16.6925
Total O&M Cost		($M)	100.155
Net Cash Flow		($M)	1553.62

The profitability of the project is the main decision-making variables to evaluate the design of the EOR process. Based on the analysis in table 11, a profit of 1.55 million dollars will be achieved with the scenario of injecting 70 MMSCF/Day of CO_2 considering the properties of a hypothetical reservoir.

The main challenge of this economic analysis was the low oil prices compared to the prices in 2007, where the outcome would be extremely large considering the recovery achieved with the current proposition. In conclusion, the economic analysis with the reservoir simulation study approves the technical feasibility of the CO_2-EOR, which is demonstrated in the oil recovery, the amount of CO_2 used for injection, the operating cost, and the time required for process.

Chapter 5

CONCLUSTION

In conclusion, the intend of this project is to apply measures in order to control the concentration of CO_2 emission in the atmosphere, which is done by efficiently capturing CO_2, and then sequester it or utilize it for industrial applications.

In this project, three main CO_2 capture methods are compared for coal fired power plant in Indiana region. Among different kinds of post-combustion methods, chemical absorption was turned out to be the best for its relatively low capital cost, easy implementation, and technical feasibility. The effects of the chemical absorption capture process were investigated referring 600MW coal-fired power plant in Indiana region. The results showed that the power plant efficiency dropped by 4~5% with capturing 42% of CO_2 coming out of the plant. Electricity production cost increased by 46% mainly due to the capital charge for CO_2 capture component and the operation and maintenance cost. The estimated CO_2 capture cost was \$48.6/ton of CO_2 avoided. In addition to the cost of capturing, there would be cost of sequestration as well.

In the study carried, different methods for sequestration were also studied and applied to sequester the large amount of CO_2 captured in the coal fired power plant. A fraction of the amount of CO_2 captured is utilized to recover the additional oil from a hypothetical reservoir in Pennsylvania. By the application of CO_2 an additional recovery of 35.8% was observed with an additional profit of \$1.55 million. It was also seen that the process is economical with an injection flow rate of 70 MMSCF/day with which the breakthrough time is 5 years. The part of the CO_2 left after using it for EOR, the rest was sequestered in geologic sites. 38.24% of the total CO_2 captured is sequestered in the hypothetical exhausted oil field in Pennsylvania. In the study, it was found that \$7.714/ ton of CO_2 should be charged in order to recover the capital cost of transportation and make the process economically feasible. It was also found that saline aquifers can also be used efficiently to sequester the gas. Sequestration costs highly depend on the transportation distance, aquifer/reservoir depth, caprock pressure, thickness, porosity and the permeability of the aquifer/reservoir.

Considering the ten year long project life, our result showed that CO_2 capture and sequestration(CCS) process cost \$53.3/ton of CO_2 captured. Although CCS charges much extra money for its implementation, it will be economically feasible with proper governmental regulations for CO_2 emission such as CO_2 tax, and CO_2 cap-and-trade.

Chapter 6

REFERENCE

1.1 http://www.eia.doe.gov/bookshelf/brochures/greenhouse/Chapter1.htm

1.2 Bryant S.: ”Geologic storage – Can the oil and gas industry help save the planet”, Society of Petroleum Engineers J., September 2007, 98-105

2.1 Davison J, Performance and costs of power plants with capture and storage of CO2. IEA Greenhouse Gas R&D Programme, Cheltenham, GL52 7RZ, UK. Received 23 February 2006

2.2 Rao A, Rubin E, A technical, economic, and environmental assessment of Amine-based CO2 capture technology for power plant greenhouse gas control in Environ. Sci. Technol. 2002, 36, 4467-4475. Department of Engineering and Public Policy, Carnegie Mellon University

2.3 Feron P H M, Hendriks C A, 2005. CO2 capture process principles and costs. Oil and Gas Science and Technology-Rev, IFP 60(3): 451–459.

2.4 Yang H, Xu Z, Fan M, Gupta R, Progress in carbon dioxide separation and capture : A review. Department of Chemical and Materials Engineering in Journal of Environmental Sciences 20(2008) 14–27, University of Alberta, Edmonton, AB, T6G 2G6, Canada. E-mail: hongqun@ualberta.ca, School of Materials Science and Technology, Georgia Institute of Technology, Atlanta, GA, 30332, USA, Gas Technology Institute, Des Plaines, IL 60018, USA, Western Research Institute, Laramie, Wyoming, 82072, USA, Oak Ridge National Laboratory, P.O. Box 2008, Oak Ridge, TN 37831, USA

2.5 Figueroa J, Fout T, Plasynski S, McIlvried H, Srivastava R, Advances in CO2 capture technology – The U.S Department of Energy’s Carbon Sequestration Program in international journal of greenhouse gas control 2 (2008) 9–20. National Energy Technology Laboratory, U.S Department of Energy, Pittsburgh, PA, United States, Science Applications International Corporation, National Energy Technology Laboratory, Pittsburgh, PA, United States

2.6 Bounaceur R, Lape N, Roizard D, Vallieres C, Favre E, Membrane processes for post-combustion carbon dioxide capture: A parametric study. Laboratoire des Sciences du Ge´nie Chimique UPR CNRS 6811, Groupe ENSIC, INPL, 1 rue Grandville, BP 541, 54001 Nancy, France Received 28 July 2005

2.7 Elwell L C, Grant W S, 2006. Technology options for capturing CO2-Special Reports. Power 150(8)

2.8 White CM. Separation and capture of CO2 from large stationary sources and sequestration in geological formations. J Air Waste Manage Assoc 2003;53:645–715.

2.9 Murai S, Fujioka Y, Challenges to the Carbon dioxide Capture and Storage (CCS) Technology in TRANSACTIONS ON ELECTRICAL AND ELECTRONIC

ENGINEERING IEEJ Trans 2008; 3: 37–42
2.10 IPCC, 2005. IPCC Special Report on Carbon Dioxide Capture and Storage. Cambridge University Press: New York, 2005
2.11 Abu-Zahra M, Niederer J, Feron P, Versteeg G, CO2 capture from power plants Part II. A parametric study of the economical performance based on mono-ethanolamine in international journal of greenhouse gas control 1 (2007) 135 – 142
2.12 Notz R, Asprion N, Clausen I, Hasse H, Selection and pilot plant tests of new absorbents for post-combustion carbon dioxide capture in Trans IChemE, Part A, April 2007
2.13 Pehnt M, Henkel J, Life cycle assessment of carbon dioxide capture and storage from lignite power plants in international journal of greenhouse gas control 3(2009)49–66
2.14 Ho M, Leamon G, Allinson G, Wiley D, Economics of CO2 and Mixed Gas Geosequestration of Flue Gas Using Gas Separation Membranes IN Ind. Eng. Chem. Res., 2006, 45 (8), 2546-2552 • DOI: 10.1021/ie050549c
2.15 Lee S, Park J, Song H, Maken S, Filburn T, Implication of CO2 capture technologies options in electricity generation in Korea in Energy Policy 36 (2008) 326–334
2.16 Soosaiprakasam I, Veawab A, Corrosion and polarization behavior of carbon steel in MEA-based CO2 capture process in international journal of greenhouse gas control 2(2008)553–562
2.17 Hendriks C, Carbon dioxide removal from coal-fired power plant, Kluwer Academic Publishers, 1994
2.18 Sakwattanapong R, Aroonwilas A, Veawab A, Kinetics of CO2 Capture by Blended MEA-AMP, Faculty of Engineering, University of Regina, Regina
2.19 Pennsylvania and coal - SourceWatch
2.20 U.S. Electric Power Industry Estimated Emissions (EIA-767 and EIA-906)
3.1 http://www.eia.doe.gov/bookshelf/brochures/greenhouse/Chapter1.htm
3.2 Bryant S.: ”Geologic storage – Can the oil and gas industry help save the planet”, Society of Petroleum Engineers J., September 2007, 98-105
3.3 http://www.energy.gov/sciencetech/carbonsequestration.htm
3.4 http://fossil.energy.gov/programs/sequestration/terrestrial/
3.5 Nguyen D.N.: “Carbon Dioxide Geological Sequestration: Technical and Economic Reviews”, SPE/EPA/DOE Exploration and Production Environmental Conference, March 2003
3.6 Sobers, L.E., Frailey, S.M. and Lawal, A.S.: ”Geological Sequestration of Carbon Dioxide in Depleted Gas Reservoirs”, SPE/DOE Symposium on Improved Oil Recovery, April 2004
3.7 Mamora, D.D. and Seo, J.G.: ”Enhanced Gas Recovery by Carbon Dioxide Sequestration in Depleted Gas Reservoirs”, SPE Annual Technical Conference and Exhibition, September 2002
3.8 Halloway, S. and van der Straaten, R.: “The Joule II project – The underground disposal of Carbon Dioxide,” Energy Conversion and Management, Vol. 36, No. 6-9, 519-522, 1995

3.9 Hendriks C.A. and Blok K.: "Underground Storage of Carbon Dioxide," Energy Conversion and Management, Vol. 36, No. 6-9, 539-542, 1995

3.10 Li Z., Dong M., Li S., Huang S.,: "CO2 sequestration in depleted oil and gas reservoir – caprock characterization and storage capacity," Energy conversion and management, Aug 2005

3.11 Rajesh J. Pawar, Norm R. Warpinski, John C. Lorenz, Robert D. Benson, Reid B. Grigg, Bruce A. Stubbs, Philip H. Stauffer, James L. Krumhansl, Scott P. Cooper, and Robert K. Svec, "**Overview of a CO 2 sequestration field test in the West Pearl Queen reservoir, New Mexico** (in Characterization of sites for geological storage of CO2)," Environmental Geosciences (September 2006), 13(3):163-180

3.12 Bachu S., " Evaluation of CO2 sequestration capacity in oil and gas reservoirs in the western Canada sedimentary basin," Alberta geological survey, Alberta Energy Research Institute (March 2004)

3.13 J. Q. Xu, G Weir, L. Paterson, I. Black, and S. Sharma," A case study of Carbon Dioxide well test," APPEA Journal, (2007)

3.14 Baines, S., Worden, R., "Geological Storage of Carbon Dioxide", Geological Society, London, 2004

3.15 Bachu, S., Bonijoly, D., and Bradshaw, J., " CO2 storage capacity estimation: Methodology and gaps", International Journal of Greenhouse Gas Control,Vol., No.4, 430-443, October 2007

3.16 Essendelft, D., Taron,J.,and Fitzgerald, M., "CO2 Sequestration through Deep Saline Injection and Photosynthetic Biological Fixation: System Design for Two Plausible CO2 Sequestration Strategies", The Pennsylvania State University

3.17 Jacobs, M., "Measurement and modeling of thermodynamic properties for the processing of polymers in supercritical fluids", Eindhoven University of Technology, Eindhoven, 2005

3.18 http://www.dcnr.state.pa.us/info/carbon/documents/GeologicalAssessment.pdf, Pennsylvania Geological Survey

3.19 http://www.beg.utexas.edu/environqlty/co2seq/co2data/0oriskany.htm , Bureau of Economic Geology, The University of Texas at Austin

3.20 Shafeen, A., Croiset, E., and Douglas,P.," CO2 sequestration in Ontario, Canada. Part II: cost estimation ", Energy Conversion and Management, Vol.45, No.20, 3207-3217, December 2004

3.21 Soong,Y., Jones, J., and Harrison, D."Mineral Trapping of CO2 with Oriskany Brine", U.S. Department of Energy, National Energy Technology Laboratory,

3.22 Jordanov, J. "Problems of CO2 Sequestration in Geological Structures", Black Sea Regional Energy Center, 2007

3.23 Dilmore, R., Lu, P. and Allen, D., "Sequestration of CO2 in Mixtures of Bauxite Residue and Saline Wastewater", Energy Fuels, Vol. 22, No.1, 343-353, 2008

3.24 Kumar, A., Noh, M., and Pope, G., "Reservoir Simulation of CO2 Storage in Deep Saline Aquifers", SPE Journal, SPE 89343, April 2004.

3.25 Meggyesy, S.D, Jagucki, P.E., and Gerst, J.,"Case Study: Evaluation of Regional Lithology for Carbon Dioxide Storage Using a Single Test Well in Southern Ohio", SPE Journal, SPE 117591, October 2008.

3.26 Izgec, A., Demiral, B., and Bertin, H., "Experimental and numerical Modeling of

Direct Injection of CO2 Into Carbonate Formations", SPE Journal, SPE 100809, September 2006.
3.27 Essendelft, D.V., Taron, J., and Fitzgerald, M., " CO2 Sequestration through Deep Saline Injection and Photosynthetic Biological Fixation: System Design for Two Plausible CO2 Sequestration Strategies", Department of Energy and Geo-Environmental Engineering, the Pennsylvania State University
3.28 Bryant, S.L., Martin, P.F., and Mcgrail, B.P, "Use of Forced Mineral Trapping for Sequestration of CO2", Pacific Northwest National Laboratory
3.29 Shafeen, A., Croiset, E., and Douglas P., "CO2 Sequestration in Ontario, Canada. Part 2: Cost estimation", energy conversion and Management, Vol. 45, No 20, 3207-3217, December 2004
3.30 Snead Mark, " The Economics of deep Drilling in Oklahoma", Oklahoma state University, February 2005
3.31 Mccoy, S., Rubin, E., " An Engineering- Economic Model of Pipeline Transport of CO2 with Application to Carbon Capture and Storage", International Journal of Greenhouse Gas Control, No 2, 219-229, 2008
3.32 Bourgoyne, A., Keith, M., and Young, F., " Applied Drilling Engineering",SPE Textbook series, Vol. 2
3.33 Ertekin, T., "Principles of Well Testing and Evaluation
3.34 Hangx, S., "Behaviour of the CO2-H2O System and Preliminary Mineralisation Model and Experiments, Utrecht University, Dec. 2005
3.35 Gaus, I., Azaroual, M., and Czernichowski, I., "Reactive Transport Modelling of the Impact of CO2 Injection on the Clayey Cap Rock at Sleipner (North Sea)", Chemical Geology, Vol, 217, No 3-4, 319-337, 25 April 2005
3.36 http://www.csudh.edu/oliver/chemdata/data-ksp.htm
3.37 Butler, J., "Carbon Dioxide Equilibria and Their Applications"
4.1 Enhance Oil Recovery Scoping Study , EPRI, (www.energy.ca.gov/process/pubs/electrotech_opps_tr113836.pdf)
4.2 www.en.wikipedia.org/wiki/Oil_reservoir
4.3 Ahmed, T. Reservoir Engineering Handbook, Gulf Publishing CO., 2000
4.4 The benefit of Recycling, www.ezinearticle.com/?The-Benefits-of-Recycling&id=605556
4.5 U.S. Department of Energy, Basin Oriented Strategies for CO2 Enhance Oil Recovery:
Illinois and Michigan Basin of Illinois, Indiana, Kentucky and Michigan, 2006 (http://www.fossil.energy.gov/programs/oilgas/publications/eor_co2/Illinois_&_Michigan_Basin_Document.pdf)
4.6 F.M. ORR, JR., J.P. Heller and J.J. Taber, Carbon Dioxide Flooding for Enhanced Oil Recovery: Promise and Problems, New Mexico Petroleum Recovery Research Center, (http://www.springerlink.com/content/g691l73n42665170/fulltext.pdf)

Appendix A

Engineering Approach

A 8575 cell model was constructed containing the basic grid information for the simulation model. The simulation model was built on 300 x 300 feet grids and contains 35 rows, 35 columns, and 7 layers. In addition to the geometric description of each cell, the model contains estimates of permeability and porosity from FAL log and core data. The construction of the model was processed according to the following steps:

1) Digitize the structure map
2) Review/analyze FAL log and core data
3) Review the distribution of the lithology beds
4) Create layer structure from FAL log and core data
5) Populate porosity and permeability
6) Initialize the model
7) Run sensitivity cases

In the beginning, a field in New Mexico was chosen for its rich data, to reflect a hypothetical reservoir in Pennsylvania for the purpose of injecting CO_2 for EOR and sequestration purposes. The structure map was digitize with the available resources to create a representable simulation model that reflects the actual field in terms of structure, top depths, and well distributions. Figure 40 represents the West Pearl Queen Reservoir in New Mexico .

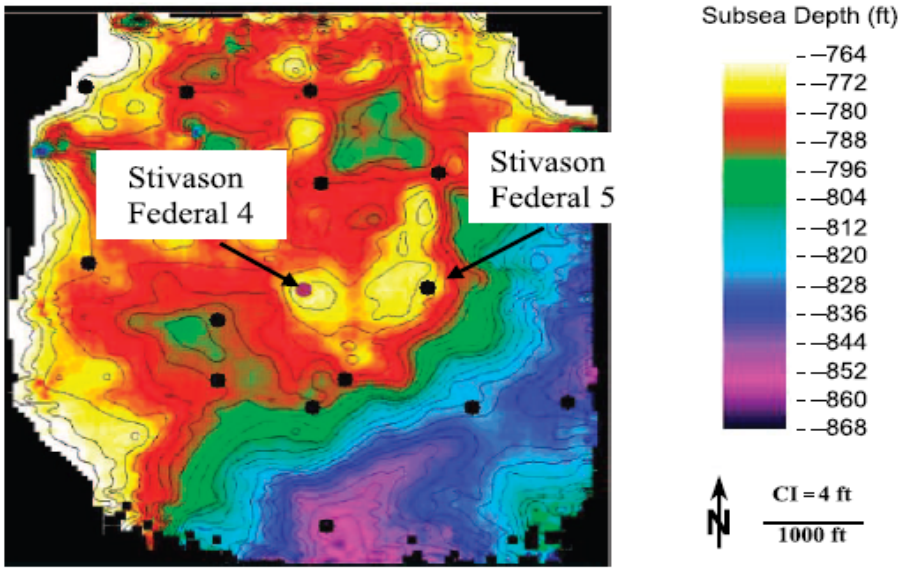

Figure 40: Structure map of West Pearl Queen Reservoir[Rajesh et al., (2006)]

The reservoir, shown in Figure 40, is divided into square blocks and the Cartesian grid system is imposed to study the EOR and CO_2 sequestration process numerically. The whole reservoir is divided into 1225 blocks for each of the seven layers. Out of these seven layers 3 layers are impervious. During numerical simulations, all the seven layers will be studied but permeable rocks are assigned rock properties as shown in Table 1 (reservoir parameters) Top view of the first layer of reservoir after imposing the grid system is shown in Figure 41. All the seven layers are assumed to have same structure.

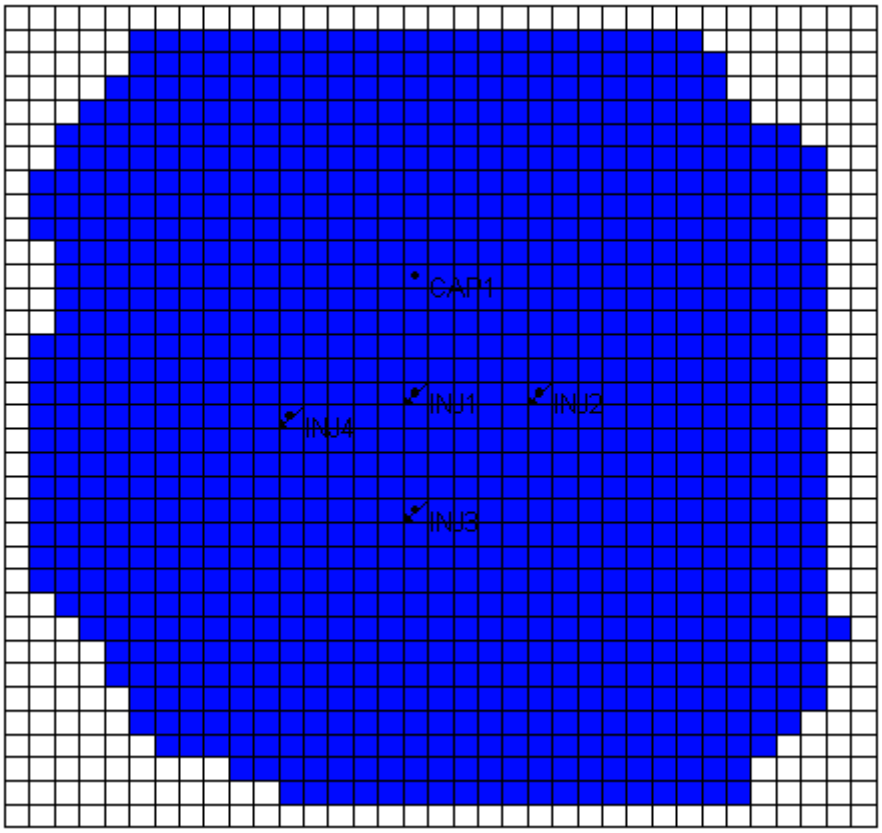

Figure 41: Simulated map of West Pearl Queen Reservoir

Each layer of the reservoir has different thickness which is calculated from the FAL plots. Since the data is available for selected points in the literature, it is assumed that each block within a layer has same thickness [Rajesh et al., (2006)]. The reservoir is assumed to be homogeneous in the horizontal plane and an-isotropic in the vertical plane. Porosity and permeability of each layer are shown in Table 1.

Table 12: Parameters of the reservoir for each layer

Layer	Top Depth (ft)	Thickness (ft)	Porosity	Permeability(md)
1	4507	16	0.1373	104
2	4523	5	0	0
3	4528	12	0.1622	320

4	4540	3	0	0
5	4543	6	0.075	10
6	4549	2	0	0
7	4551	6	0.075	10

FAL log was processed and calibrated against the core data to add more creditability to the analysis of the data and to the calculation of the pore volume. It also assesses the up scaling of the model to provide an estimated value of the number of layers that reflects the characteristics of the formation.

The parameter curves of the FAL log and core data provided different information, such as gamma ray, porosity, and permeability values. The gamma ray peaks indicate the presence of a layer boundary, the value and direction of the peak indicates the type of transition (resistive–conductive or conductive–resistive). The peaks identify the zones that are mostly to contain hydrocarbon, which helps in combining layer configurations together to present the field characteristics with less number of layers. Figure 42 represent the processing of the calibrated FAL log and core data.

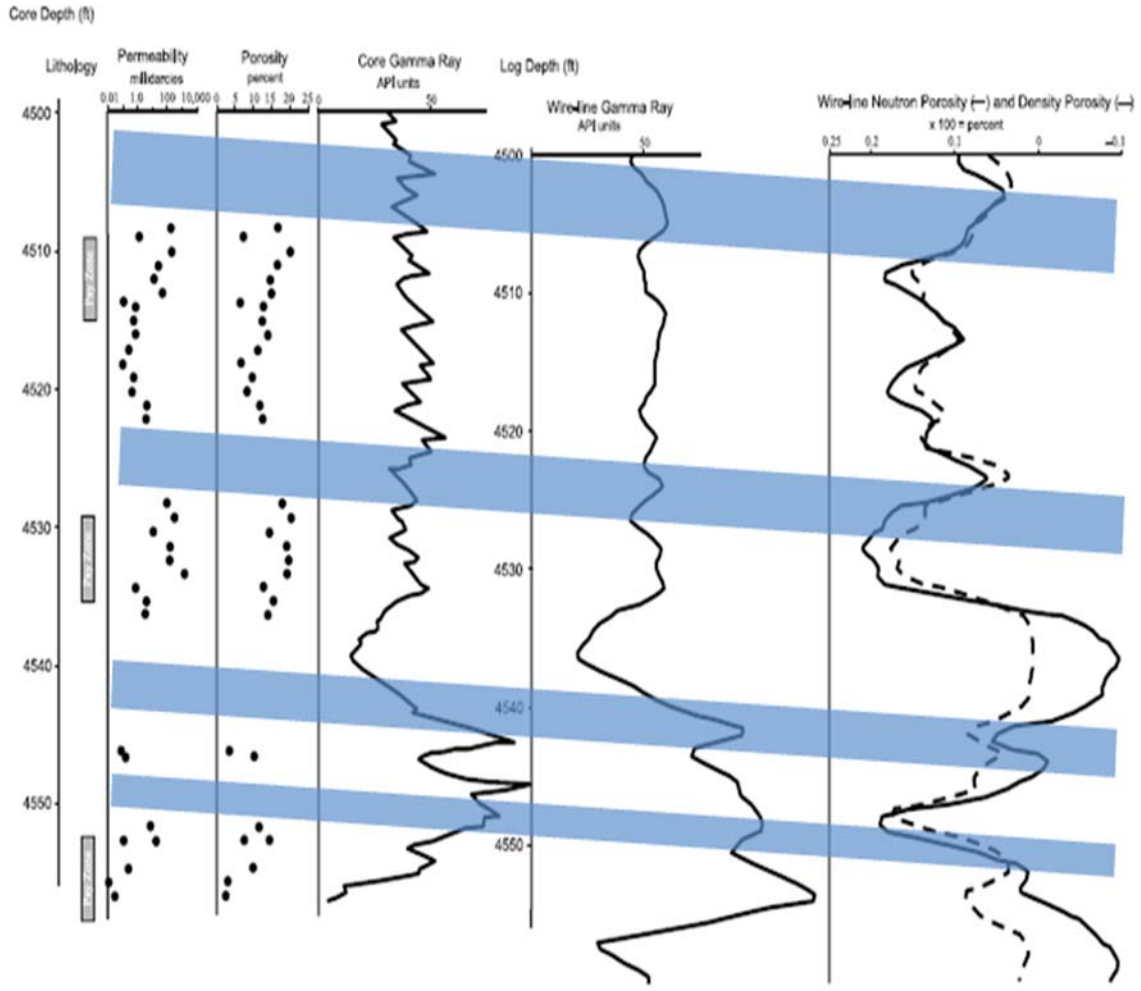

Figure 42: Processing of FAL log and core data

Porosity and permeability were populated across the reservoir based on the core data and the layering scheme. It was assumed the non-reservoir layers have no permeability and porosity to limit the contribution of production to the reservoir layers. Table 8 represents the parameters of the field per layer.

Appendix B

CO_2 Sequestration In Saline Aquifer

B.1 Transportation

- Inlet Pressure:10350kPa (around 1500psia)
- Outlet Pressure:10000kPa (around 1500psia)
- Transportation distance: 100 km (6.2 miles)
- Pipeline roughness: 0.0457mm (A typical steel pipeline value [3.26])
- Compressibility factor: 0.2166 (Peng-Robinson)
- Mass flux: 32kg/s (70.41lbs/s)
- Temperature: 20˚C

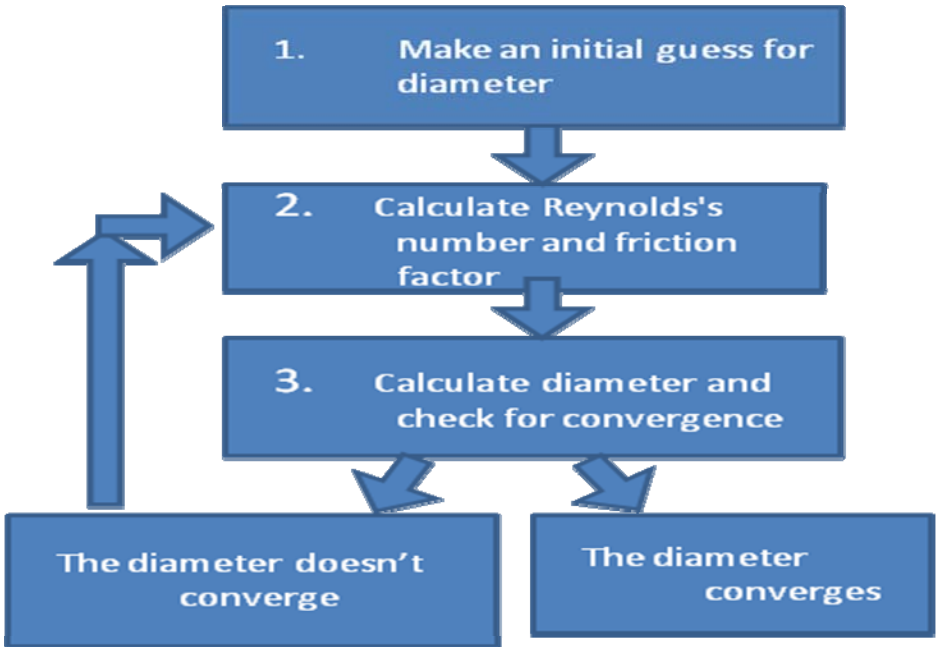

Figure 43: Diameter calculations procedure

Below, we can quantify the Reynolds's number.

$$Re = \frac{4\,m}{\mu\,\pi\,D} \qquad (1)$$

Where:

- m: mass flux (kg/s)
- μ: viscosity (Pa.s)
- D: Diameter (m)

Viscosity can be assumed as the viscosity value at 293.15˚K which is $14.8*10^{-6}$ Pa.s for CO_2.

Calculation of diameter requires the compressibility factor. The compressibility factor for that pressure and temperature can be calculated using Peng-Robinson. This requires the critical pressure (1072.8psia), critical temperature (547.47˚K) and the acentric factor (0.239) values.

Peng Robinson correlation can be written in this way:

$$P = \frac{R\,T}{V_m - b} - \frac{a\,\alpha}{V_m^2 + 2\,b\,V_m - b^2} \qquad (2)$$

The unknowns can be quantified as below: a, b, V_m are the other coefficients which can be calculated from some equations which are written in any thermodynamic book.

$$a = \frac{0.45724\, R^2\, T_c^2}{P_c} \quad , \quad b = \frac{0.0778\, R\, T_c}{P_c}$$

$$\alpha = \left(1 + (0.37464 + 1.54226\,\omega - 0.26992\,\omega^2)(1 - T_r^{0.5})\right)$$

$$T_r = \frac{T}{T_c} \quad , \quad V_m = \frac{M}{\rho}$$

- Vm = Molecular Volume
- M= Molecular weight, Mco2=44.1
- ω is the acentric factor: It is 0.228 for CO_2

Now, we can calculate the frictional factor using the below equation [3.26] :

$$\frac{1}{2\sqrt{f_F}} = -2.0 log\left\{\frac{\varepsilon/D}{3.7} - \frac{5.02}{R_e}\log\left[\frac{\varepsilon/D}{3.7} - \frac{5.02}{R_e}\log\left(\frac{\varepsilon/D}{3.7} + \frac{13}{R_e}\right)\right]\right\} \qquad (3)$$

Lastly, we can calculate the new diameter [3.26].

$$D = \sqrt[5]{\frac{-64\, Z^2 R^2 T^2\, f_F\, m^2 L}{\pi^2 \left[M Z R T \left(P_2^2 - P_1^2\right)\right]}} \qquad (4)$$

If this D value matches with the initial D guess, then we can take it as our diameter. However, if it doesn't converge we need to do the same steps again until it converges. Calculations are coded in Matlab.

B.2 Formation Fracture Pressure

There are several calculations. Firstly, weight of overburden needs to be calculated with below formula [3.27]:

$$\sigma_{ob} = \rho g D - \frac{(\rho - \rho_{fl})g\emptyset}{K}(1 - \exp(-K D)) \qquad (5)$$

- σ_{ob} =weight of overburden (psi)
- ρ=grain density (2.11g/cm^3) (from Table) [3.27]
- g=gravitational accelaration(9.81m/s^2)
- D=Depth1000ft (reservoir data)
- ρ_{fl} =pore fluid density 1g/cm^3 (assumption from a similar example) [3.27]
- Ø=porosity (0.1-reservoir data)

- K=porosity decline constant (0.000085ft^{-1} -from an example) [3.27]

Right hand side has 2 pieces. the first one shows the effect of the depth and the density. The 2nd one is very small. It takes the reduction of the porosity with depth into account. The weight of overburden is found to be 5152psig

Using the Eaton Correlation, fracture pressure can be calculated. First, matrix stress needs to be found [3.27].

$$\sigma_{min} = \frac{\mu}{1-\mu}\sigma_z \quad (6)$$

- σ_{min}=minimum matrix stress (psia)
- μ=poisson's ratio (0.3 taken from a table for 10000ft depth) [3.27]
- σ_z=matrix stress (=overburden weight-pore pressure (psig))

Pore pressure is taken as 3000psig after making comparison with an example. finally minimum matrix stress is found as 922 psig

Lastly, fracture pressure can be calculated by summing minimum matrix pressure and overburden weight as 6704 psig=6718psia. [3.27]

$$p_{ff} = \sigma_{min} + \sigma_{ob} \quad (7)$$

B.3 Pressure Profile

The injection rate is 32 kg/s (70.4 lbs/s). Fracture pressure is 6718 psia. Our formation pressure is 3000 psia.

The pressure profile can be calculated with below equations: [3.28]

$$\Delta P_d = \frac{1}{2}\mathrm{Ei}\left(-\frac{r_d^2}{4t_d}\right) \quad (8)$$

ΔPd=Dimensionless Pressure
rd= Dimensionless radius
td= Dimensionless time

$$\Delta P_d = \frac{P_i - P}{P_i + q_d} \quad (9)$$

Where:

Pi= Initial pressure (psia)
P: Final Pressure (psia)
q_d:Dimensionless flow rate (STB/D)

$$r_d = \frac{r}{r_w} \quad (10)$$

r: Distance from the wellbore (ft)
r_w: wellbore radius (ft)

$$t_d = \frac{2.637 \times 10^{-4} \times k \times t}{\phi \mu \, c \, r_w^2} \quad (11)$$

k: permeability (md)
t: time(hr)
ø : Porosity
μ: viscosity: (cp)
c: compressibility ($psia^{-1}$)

$$q_d = \frac{141.2 \, B \, q \, \mu}{k \, r \, p_i} \quad (12)$$

q: Flowrate STB/D
B: Bulk volume factor

Flowrate is known. It can be converted from lbs/ year to STB/D as 8783127 STB/D. Viscosity (0.056cp) and compressibility ($8.46*10^{-5}$ $psia^{-1}$) can be calculated from tables and charts [3.28]. Porosity and permeability of the reservoir are known . Bulk volume factor [1/285 RB/SCF] is density in standard conditions/ density in reservoir conditions. Using these calculations, pressure increase with time at different locations can be calculated assuming radial flow, constant flow rate, constant properties.

B.4 Hydrodynamic Trapping

The reservoir density is known (Peng- Robinson) . We need to calculate how much free space we have in a unit volume. The free volume to be trapped can be calculated with below formula:

$$V_{free} = V \, \emptyset \, (1 - S_{wirr}) \quad (13)$$

- V_{free}: Unit volume where gas can be sequestrated
- V: Unit volume
- ø: Porosity
- S_{wirr}: Irreducible water Saturation.

Porosity is 0.1 and S_{wirr} is assumed as 0.2. Finally, when we multiply the free space with the density we can find the mass which can be sequestrated in a unit volume as 37.2 kg/m^3 (2.32 lbs/ft^3).

B.5 Solubility Trapping

Using the below equation, we can calculate how much CO_2 can be sequestrated in a unit volume. [3.11]

$$X_b^{CO_2} = X_w^{CO_2}\,(1 - 4.893414 * 0.01S + 0.0013028838\,S^2 + 0.00001871199\,S^3 \quad (14)$$

- X_b^{CO2} , X_p^{CO2} : Solubility of CO_2 in brine and pure water [g/lt]
- S: Salinity in mass fraction

Using the below equation we can find how much CO_2 can be sequestrated totally [3.10].

$$Vco2t = Ah\emptyset(1 - Swirr) \quad (15)$$

where A is the trap area, h is the thickness, $\emptyset$ is porosity and Swirr is the irreducible water saturation.

Everything is known except for the solubility of CO_2 in pure water. It can be calculated with below formula [3.29].

$$\ln\left(\frac{f_{CO_2}}{x_{CO_2}}\right) = \ln H_{CO_2}^{*} + \frac{V^{-\infty}_{CO_2}}{RT}\,P \quad (16)$$

- X_{CO_2} : Solubility of CO_2 in pure water
- $H_{CO_2}^{*}$: Henry's Constant for CO_2 (29.41 L. atm/mol)
- $V^{-\infty}_{CO_2}$: Molar volume of CO_2 at infinite dilution in water: 0.033mol/L
- f_{CO_2} : Fugacity of CO_2

Fugacity of CO_2 can be quantified according to its pressure and temperature as below [3.38].

$$f_{CO_2} = b_1 + \left[b_2 + b_3\,T + \frac{b_4}{T} + \frac{b_5\,P}{(T-150)} + \left[b_6 + b_7\,T + \frac{b_8}{T}\right] + \left[b_9 + b_{10}\,T + \frac{b_{11}}{T}\right]\ln P + \frac{[b_{12} + b_{13}\,T]}{P} + \frac{b_{14}}{T} + b_{15}\,T^2 \quad (17)$$

'*b*' values are parameters which change according to the pressure and temperature interval. for this, project the best values for b can be found in below Table 9.

Table 13: Coefficients for fugacity of CO2

b1	1	b6	-3.83891E-06	b11	0
b2	0.00475868	b7	0	b12	0
b3	-3.357E-06	b8	0.00228151	b13	0
b4	0	b9	0	b14	0
b5	1.3179396	b10	0	b15	0

B.6 Mineral Trapping

Precipitation rate can be calculated with below formula [3.36]:

$$r = kA\left[1 - \left(\frac{Q}{K}\right)\right] \quad (18)$$

Where:

- r is the dissolution/precipitation rate
- A is the specific reactive surface area per kg H2O
- k is the rate constant (moles per unit mineral surface area and unit time)
- K is the equilibrium constant for mineral water reaction written for one mole
- Q is the ion activity product
-

The unknowns of the r_m function such as Q, K, k and A need to be found. Rate constant (k) can be found with below formula[3.11]:

$$k = k_{25} \exp\left(-\frac{E_a}{R}\left(\frac{1}{T} - \frac{1}{298.15}\right)\right) \quad (19)$$

This equation is to adjust the rate constant according to the temperature. Because our temperature is close to normal conditions, we can take k_{25} as our k.

Q value can be calculated by taking the ratio of the molarity of the right hand side of the chemical equilibrium divided by the product of the left hand side. Here, because of the low availability of the data, molarities of the final product is assumed as 10^{-7} mol/. However, the

molarities of the minerals are known so that ion activity of the products can be calculated. Finally the coefficients are given in Table 10.

Table 14: Mineralization Capacity

	MW	K	Am(m^2/g)	Q	Rate Constant(mol/m2/s)	Ea(J/mol)
Calcite	100	3.8*10^-9[3.32]	6.71e−2 [3.30]	4.77E-05	1.4*10^-9 [3.30]	7000 [3.30]
Dolomite	184.42	10^-17[3.33]	6.35*10^-2 [3.31]	0.022601836	2.951*10^-8 [3.30]	52200 [3.30]
Siderite	115.86	3.2*10^-11[3.32]	4.61e−2 [3.30]	0.001014545	1.26*10^-9 [3.30]	62760 [3.30]
Magnesite	84.3	3.5*10^-8[3.32]	6.04*10^-2 [3.31]	4.73E-05	4.571*10^-10 [3.30]	23500 [3.30]

B.7 Leakage

The leakage through the caprock can be calculated with below formula [3.11]:

$$Q_{leak} = \frac{k\, k_r A\, \Delta\rho g h}{\mu \Delta z} \quad (20)$$

where, Q is leakage rate through the caprock, k is absolute permeability of the caprock, kr is the relative permeability of CO_2, A is the cross sectional area, μ is CO_2 viscosity, g is the gravity acceleration, $D\rho$ is the density difference between water and CO_2, and h is the height of CO_2 column.

Permeability is assumed as $10^{-18}m^2$, relative permeability is assumed 0.3. Sequestration in pore space is 37.2 kg/m^3. for 50 years, we will sequestrate $50*10^7$ tons of CO_2. If the thickness is 40 ft, the cross-sectional area can be calculated as 50 km^2. Viscosity is 0.056 cp. finally, we can calculate the Q leakage as $2.62*10^{-6}$kg/s (0.000113% of total CO_2) which is insignificant.

B.8 Transportation Cost

Transportation cost is a function of length and diameter [3.26].

.

$$\log(C) = a + b \times \log(L) + c \times \log(D) \quad (21)$$

Where:

- L: Pipeline length(10km)
- D: Diameter (inch)
- C=Capital Cost ($)

This equation need to be applied for all 4 types of different parameters of transportation cost such as ROW, Labor, Miscellaneous and Material costs. These values are listed for North-Eastern USA in Table 11

Table 15: Coefficients for Transportation

Coefficient	Materials	Labor	ROW	Miscellaneous
a	3.112	4.562	3.95	4.39
b	0.901	0.82	1.049	0.783
c	1.59	0.94	0.403	0.791

Appendix C

MATLAB Codes for CO2 Sequestration in Saline Aquifers

C.1 Pressure Profile

```
clc
clear
t=[0.1,1,10,1000,1000000];
r=0.25:0.25:5000;
rw=0.25;
gamma=2.637*10^-4;
per=14.1;
por=0.1;
mu=0.056;
c=8.46*10^-5;
B=1/234.85;
X=[-5000:100:5000];
Y=[-5000:100:5000];

q=8783127; %%%%% 32kg/s
q=q.*40/32;
% q=q.*0.75
q=q/2;

[x,y]=meshgrid(X,Y);


for k=1:5
capX(:,:,k)=(rw^2.*por*mu*c*(x.^2+y.^2))./(4*2.637*10^-4*k.*t(k));
end

eigen=expint(capX);
dP=141.2*q*mu*B/(per*40)*0.5.*eigen;

for k=1:5
capX2(:,:,k)=(por*mu*c*((x-2000).^2+y.^2))./(4*2.637*10^-4*k.*t(k));
end
eigen2=expint(capX2);
dP2=141.2*q*mu*B/(per*40)*0.5.*eigen2;
%

d=dP+dP2;%+dP3+dP4%+dP5+dP6+dP7+dP8+dP9+dP10;
Pi=3000;
```

```
P=Pi+d;
P1=P(:,:,1);
P2=P(:,:,2);
P3=P(:,:,3);
P4=P(:,:,4);
P5=P(:,:,5);
surf(x,y,P1);
surf(x,y,P2);
surf(x,y,P3);
surf(x,y,P4);
surf(x,y,P5);
```

C.2 Peng Robinson

```
function [dens,Z] = density(T,P,Pc,Tc,acentric)

%%%Calculation of density. Use Peng Robinson
%%%Characteristics for water
%%%
% Pc=3200;
% Tc=1164;
% acentric=0.344;


m1 = 1 + sqrt(2);
m2 = 1 - sqrt(2);
atta = 0.457235529;
attb = 0.077796074;


m = 0.374640+acentric.*1.5422-(acentric.^2)*0.26992;

Tr = T/Tc;
Pr = P/Pc;
B = attb*Pr/Tr;
X = atta*Pr/(Tr^2);
Y = 1 + m*(1 - sqrt(Tr));
Y = Y^2;
A = X*Y;

st = B*(m1 + m2 -1)-1;
nd = A + m1*m2*B^2 - (m1+m2)*B*(B+1);
rd = A*B + m1*m2*B^2*(B+1);
Kokbulma = [1 st nd -rd];
z = roots ( Kokbulma);
n=0;
for i =1:3
if isreal(z(i))==1
n = n+1;
```

```
elseif isreal(z(i))==0
n = n;
end

if n==1 & isreal(z(i))==1
Z = z(i);
elseif n ==2 & isreal(z(i))==1
Z1 = Z;
Z2 = z(i);
if Z1 > Z2
Zmin = Z2;
Zmax = Z1;
elseif Z1 < Z2
Zmin = Z1;
Zmax = Z2;
end
elseif n==3 & isreal(z(i))==1
Zmin =min(real(z));
Zmax=max(real(z));

end
end

if n==2||n==3
dGRT = (Zmax - Zmin)+log((Zmin-B)/(Zmax-B))-(A/(B*(m2-
m1)))*log(((Zmin+m1*B)*(Zmax+m2*B))/((Zmin+m2*B)*(Zmax+m1*B)));
if dGRT>0
Z = Zmin;
elseif dGRT<0
Z = Zmax;
end
end

dens= 10000*44.1/(Z*8.31*293.15);
%%%%%%kg/m^3
```

C.3 Transportation and Cost Analysis

```
clc
clear
%%%%%Input
%%%%%P=10000kPa=1450psia
%%%%Temperature 20C=527.67R
T=527.67;
% P=1450;
P=3000;
Pc=1072.8;
Tc=547.47;
R=10.73;
```

```
acentric=0.239;
rough=0.0457*10^-3;
%%%%%%
%%%for gas, viscosity is independent from pressure. It changes with
%%%temperature. Our temperature is fixed to 20 celcius. for that
%%%temperature dynamic viscosity is 14.8*10^-6 Pa.s
viscosity=14.8*10^-6;
MW=44.1;
m=20:40;%%%%(kg/s)

[dens,Z] = density(T,P,Pc,Tc,acentric);

% dgallon=dens*0.008345;
% Pc=dgallon*0.1*0.8*0.052*3000;
D=ones(21,1);%%%%(m)
L=100;
for i=1:21
while(1)
Re(i)=4*m(i)/viscosity/pi/D(i);
X(i)=-2*log10(rough/D(i)/3.7-5.02/Re(i)*log10(rough/D(i)/3.7-
5.02/Re(i)*log10(rough/D(i)/3.7+13/Re(i))));

Ff(i)=1/4/X(i)^2;

%%%%Below Mohitpour et al.
%%%% L=10000? Pressure difference=1000? Assume pressure drop=35kPa/km
Dn(i)=(64*Z^2*R^2*293.15^2*Ff(i)*m(i)^2*L*1000/(pi^2*(MW*Z*8.31*293.15*(10350
^2-10000^2))))^0.2;
if abs(D(i)-Dn(i))<0.01
break
end
D(i)=Dn(i);
end
D(i)=Dn(i);
end
% %%%%%Cost Estimation
Material=10^3.112*L^0.901.*(D.*39).^1.59;
Labor=10^(4.487+0.075)*L^0.82.*(D.*39).^0.94;
ROW=10^3.95*L^1.049.*(D.*39).^0.403;
Misc=10^(4.39+0.145)*L^0.783.*(D.*39).^0.791;
Cost=Material+Labor+ROW+Misc;

% m=m.*2.2; %(lbs/s)
D= 3.280.*D; %(ft)
i=0;
for m=20:40
i=i+1;
if m<24
Costa(i)=1132700;
elseif m>=24
Costa(i)=1132700*2;
end
```

```
end


Costwell(:,1)=Costa(1,:);

Totalcost=Cost+Costwell;
%%%Interest Rate 5%, Payback 10 yrs

NPV=Totalcost.*1.1./12.25;

i=0;
for m=20:40
i=i+1;
unit(i)=NPV(i)/m/3.600/24/365;
end

m=m.*2.2;
```

C.4 Solubility Trapping

```
%%%%%%%%Solubility Trapping
clc
clear
S=[0.2,0.7,1,1.5];
b1=1;
b2=4.7586845*10^-3;
b3=-3.3569963*10^-6;
b4=0;
b5=-1.3179396;
b6=-3.8389101*10^-6
b7=0;
b8=2.2815104*10^-3;
b9=0;
b10=0;
b11=0;
b12=0;
b13=0;
b14=0;
b15=0;


%%%%Temp-Celcius, Pressure-Bar
P=2000:100:6000;
T=20;
P=P.*0.068948;
```

```
fug=b1+(b2+b3*T+b4/T+b5/(T-
150)).*P+(b6+b7*T+b8/T).*P.^2+(b9+b10*T+b11/T).*log(P)+(b12+b13*T)./P+b14/T+b
15/T^2;

%%%%%Temp-Kelvin, Pressure-atm,
fug=0.9869.*fug;
Hco2=29.41;
Vco2=0.033;
R=0.082;
P=P.*0.9869;
T=293.15;
X=log(Hco2)+Vco2/R/T.*P;
%%%Xco2(mol/L)
Xco2=fug./exp(X);
%%%Xco2(gr/L)/(kg/m^3)
Xco2=Xco2.*44.1;
for i=1:4
for j=1:41
Xbco2(j,i)=Xco2(j)*(1-4.893414*10^-2*S(i)+0.1302838.*S(i)^2+0.1871199*10^-
4*S(i)^3);
end
end

%%%%Conversion of units
%%%%bar=14.5psia
P=P.*14.5;
%%%kg/m3=0.062428lbs/ft3
Xbco2=Xbco2.*0.062428;

%%%Volume
V=1;
por=0.1;
Swirr=0.2;
Vco2=V*por*(1-Swirr);
Mcap=Xbco2.*Vco2
```